

Bicarbonate-dependent chloride transport drives fluid secretion by the human airway epithelial cell line Calu-3

Jiajie Shan¹, Jie Liao¹, Junwei Huang¹, Renaud Robert¹, Melissa L. Palmer², Scott C. Fahrenkrug², Scott M. O'Grady² and John W. Hanrahan^{1,3}

¹Department of Physiology, McGill University, Montréal, QC H3G 1Y6, Canada

²Departments of Physiology and Animal Science, University of Minnesota, St Paul, MN 55108, USA

³McGill University Health Centre Research Institute, Montréal, QC H3G 1Y6, Canada

Key points

- The mechanisms of anion and fluid transport by airway submucosal glands are not well understood and may differ from those in surface epithelium.
- The Calu-3 cell line is often used as a model for submucosal gland serous cells and has cAMP-stimulated fluid secretion; however, it does not actively transport chloride under short-circuit conditions.
- In this study we show that fluid secretion requires chloride, bicarbonate and sodium, that chloride is the predominant anion in Calu-3 secretions, and that a large fraction of the basolateral chloride loading during cAMP stimulation occurs by $\text{Cl}^-/\text{HCO}_3^-$ exchange.
- The results suggest a novel cellular model for anion and fluid secretion by Calu-3 and submucosal gland acinar cells

Abstract Anion and fluid secretion are both defective in cystic fibrosis (CF); however, the transport mechanisms are not well understood. In this study, Cl^- and HCO_3^- secretion was measured using genetically matched CF transmembrane conductance regulator (CFTR)-deficient and CFTR-expressing cell lines derived from the human airway epithelial cell line Calu-3. Forskolin stimulated the short-circuit current (I_{sc}) across voltage-clamped monolayers, and also increased the equivalent short-circuit current (I_{eq}) calculated under open-circuit conditions. I_{sc} was equivalent to the HCO_3^- net flux measured using the pH-stat technique, whereas I_{eq} was the sum of the Cl^- and HCO_3^- net fluxes. I_{eq} and HCO_3^- fluxes were increased by bafilomycin and ZnCl_2 , suggesting that some secreted HCO_3^- is neutralized by parallel electrogenic H^+ secretion. I_{eq} and fluid secretion were dependent on the presence of both Na^+ and HCO_3^- . The carbonic anhydrase inhibitor acetazolamide abolished forskolin stimulation of I_{eq} and HCO_3^- secretion, suggesting that HCO_3^- transport under these conditions requires catalysed synthesis of carbonic acid. Cl^- was the predominant anion in secretions under all conditions studied and thus drives most of the fluid transport. Nevertheless, 50–70% of Cl^- and fluid transport was bumetanide-insensitive, suggesting basolateral Cl^- loading by a sodium–potassium–chloride cotransporter 1 (NKCC1)-independent mechanism. Imposing a transepithelial HCO_3^- gradient across basolaterally permeabilized Calu-3 cells sustained a forskolin-stimulated current, which was sensitive to CFTR inhibitors and drastically reduced in CFTR-deficient cells. Net HCO_3^- secretion was increased by bilateral Cl^- removal and therefore did not require apical $\text{Cl}^-/\text{HCO}_3^-$ exchange. The results suggest a model in which most HCO_3^- is recycled basolaterally by exchange

with Cl^- , and the resulting HCO_3^- -dependent Cl^- transport provides an osmotic driving force for fluid secretion.

(Resubmitted 17 May 2012; accepted after revision 9 July 2012; first published online 9 July 2012)

Corresponding author J. W. Hanrahan: Department of Physiology, McGill University, 3655 Promenade Sir William Osler, Montréal, Québec, Canada H3G 1Y6. Email: john.hanrahan@mcgill.ca

Abbreviations ALI, air–liquid interface; ASL, airway surface liquid; CF, cystic fibrosis; CFTR, cystic fibrosis transmembrane conductance regulator; J_{net} , net $^{36}\text{Cl}^-$ flux; J_{ms} , mucosal-to-serosal $^{36}\text{Cl}^-$ flux; J_{sm} , serosal-to-mucosal $^{36}\text{Cl}^-$ flux.

Introduction

The airways are protected by a microscopic layer of airway surface liquid (ASL) which contains water, inorganic ions, lipids, mucins and proteins. The ASL humidifies inspired air and contains antimicrobial factors that defend the epithelium from inhaled pathogens. Its depth (5–30 μm in healthy airways; Widdicombe, 2002; Boucher, 2003) is reduced in cystic fibrosis (CF) due to abnormal transepithelial salt and water transport (Tarran *et al.* 2006), and this diminishes mucociliary clearance and leads to recurrent infections and inflammation. Despite the importance of ASL in airway host defense and pathophysiology, the relationship between anion and fluid secretion by airway epithelia remains poorly understood.

The cystic fibrosis transmembrane conductance regulator (CFTR) is the product of the CF gene and contributes to airway secretion. It is a phosphorylation-regulated, non-rectifying anion channel of ~ 7 pS conductance (Hanrahan *et al.* 1994), which serves as the rate-limiting step during cAMP-stimulated secretion by many epithelia (e.g. Klyce & Wong, 1977) including those in the airways (Frizzell & Hanrahan, 2011). Although the CFTR channel pore is permeable to Cl^- and HCO_3^- (Gray *et al.* 1990; Poulsen *et al.* 1994; Linsdell *et al.* 1997) and secretion of both anions is reduced in CF (Widdicombe *et al.* 1985; Smith & Welsh, 1992), the relative contributions of CFTR, SLC26A transporters and other pathways for apical HCO_3^- efflux remain controversial (Lee *et al.* 1999; Ishiguro *et al.* 2009; Kim & Steward, 2009; Garnett *et al.* 2011).

Anion secretion has been studied extensively in the human airway cell line Calu-3, which spontaneously differentiates into predominantly serous-like cells that express CFTR and antimicrobial proteins, and a smaller population of goblet-like cells, which contain mucin granules. When cultured on porous supports at the air–liquid interface (ALI), Calu-3 monolayers generate a robust basal short-circuit current (I_{sc}) that cannot be ascribed to net Cl^- or Na^+ fluxes (Shen *et al.* 1994; Haws *et al.* 1994; Shan *et al.* 2011) and is thought to be mediated by active HCO_3^- secretion (Lee *et al.* 1998). Forskolin stimulates transepithelial $^{36}\text{Cl}^-$ fluxes in both directions under I_{sc} conditions without causing detectable net Cl^- secretion, and the I_{sc} is insensitive to the

NKCC1 inhibitor bumetanide (Devor *et al.* 1999). These findings and subsequent pH-stat measurements suggest that forskolin stimulates electrogenic HCO_3^- transport under I_{sc} conditions (Devor *et al.* 1999; Krouse *et al.* 2004).

Various cellular models have been proposed to explain Calu-3 anion transport. According to one scheme, HCO_3^- secretion occurs by Na^+ -coupled entry at the basolateral membrane and exit through apical CFTR channels (Devor *et al.* 1999) and/or via pendrin-mediated apical anion exchange (Garnett *et al.* 2011). Net HCO_3^- secretion is stimulated by forskolin; therefore, the fluid produced during forskolin stimulation is expected to be alkaline. By contrast, secretagogues that hyperpolarize Calu-3 cells elicit mainly Cl^- transport, as shown by the net $^{36}\text{Cl}^-$ flux measured during stimulation by the potassium channel activator 1-EBIO (Devor *et al.* 1999). Despite much progress, the mechanisms and relationship between anion transport and fluid secretion remain uncertain in Calu-3 cells and in gland serous cells. HCO_3^- appears to be the only actively secreted anion under I_{sc} conditions, consistent with bumetanide-insensitive fluid secretion by native airway glands (Corrales *et al.* 1984), yet most studies indicate that the pH of native gland secretions and airway surface liquid is near neutrality or slightly acidic (Kyle *et al.* 1990; Coakley *et al.* 2003; Song *et al.* 2006; reviewed by Fischer & Widdicombe, 2006).

In the present study, net HCO_3^- transport was measured under open- and short-circuit conditions using an automated pH-stat, and $^{36}\text{Cl}^-$ fluxes and the volume and anion composition of fluid secreted by polarized Calu-3 monolayers were measured under comparable conditions. Forskolin-stimulated I_{sc} was identical to the net HCO_3^- flux, further evidence that net HCO_3^- transport mediates the I_{sc} as suggested previously (Devor *et al.* 1999; Ballard *et al.* 1999). However, although fluid secretion was strictly dependent on the presence of HCO_3^- , the predominant anion in the secreted fluid was Cl^- . These and other results indicate that most HCO_3^- entering the cells by basolateral cotransport with Na^+ is recycled to the basolateral side in exchange for Cl^- , and suggest a revised model in which fluid secretion is mainly driven by HCO_3^- -dependent Cl^- transport. A preliminary account of these results was presented at the 36th International Congress of Physiological Sciences, Kyoto, Japan (2009).

Methods

Cell culture

Two genetically modified Calu-3 cell lines were used: a CFTR knock-down cell line which stably expresses a 21-mer shRNA that specifically targets CFTR mRNA transcripts, and a control cell line, which expresses shRNA bearing four mutations that reduce its ability to silence *cfr* (*Sizt* and *Alter* cell lines, respectively; Palmer *et al.* 2006). Both cell lines were cultured in Eagle's minimum essential medium (EMEM; Wisent Bioproducts, St. Bruno, Qc) containing 7% fetal bovine serum (FBS). To allow comparison with previous studies, control experiments were also performed using parental Calu-3 cells (HTB-55, American Type Culture Collection, Manassas, VA, USA) cultured in EMEM containing 15% FBS.

Cells were seeded at 5×10^5 cells cm^{-2} on Snapwells (1.12 cm^2 ; Costar, Corning Life Sciences, Lowell, MA, USA) for studies of I_{sc} and HCO_3^- secretion, and at the same density on Transwells (4.67 cm^2 , Corning) for measuring fluid secretion rate and composition. Fresh medium was placed on the basolateral side 1 day after plating and the apical medium was removed to establish an air-liquid interface (ALI). Any fluid that appeared spontaneously on the apical surface was removed after 3 days. Cultures were maintained in a humidified 5% CO_2 incubator at 37°C and studied after 21–25 days. Polarization of the monolayers with respect to CFTR function was confirmed by imposing a transepithelial Cl^- gradient and measuring the forskolin-stimulated current after permeabilization of the basolateral or apical membrane with nystatin (100 $\mu\text{g ml}^{-1}$ apical; 360 $\mu\text{g ml}^{-1}$ basolateral).

Solutions and media

To measure HCO_3^- secretion under control pH-stat conditions, monolayers were mounted in modified Ussing chambers and the apical surface was bathed with unbuffered solution containing (mmol l^{-1}): 120 NaCl, 5 KCl, 1.2 MgCl_2 and 1.2 CaCl_2 . The basolateral side was bathed with 120 NaCl, 25 NaHCO_3 , 3.3 KH_2PO_4 , 0.8 K_2HPO_4 , 1.2 MgCl_2 , 1.2 CaCl_2 and 10 glucose. Nominally Na^+ -free solution was prepared by replacing NaHCO_3 with equimolar choline bicarbonate, and NaCl was replaced with *N*-methyl-D-glucamine chloride. Nominally Cl^- -free solution was prepared by replacing Cl^- salts with gluconate salts, and the $[\text{Ca}^{2+}]$ was increased from 1.2 to 4 mmol l^{-1} by adding calcium gluconate to compensate for gluconate binding. Nominally HCO_3^- -free solution was prepared by replacing 25 mmol l^{-1} NaHCO_3 with 25 mmol l^{-1} Na-Hepes and gassing with 100% O_2 . All solutions were adjusted to pH 7.4. When studying basolateral

anion exchange, pH-stat was performed on the basolateral side after permeabilizing the apical membrane with nystatin and adding 25 mmol l^{-1} NaHCO_3 on the apical side. Apical addition of choline bicarbonate gave the same result as NaHCO_3 , presumably because the current induced by the apical-to-basolateral gradient of 170 \rightarrow 145 Na^+ present after apical addition of NaHCO_3 (25 mmol l^{-1}) was obscured by sodium pump current. In control experiments, osmotic gradients produced by adding 50 mmol l^{-1} mannitol on the apical side had no effect on I_{eq} or HCO_3^- flux. In pH-stat experiments, the unbuffered side was stirred with 100% O_2 while the opposite side containing HCO_3^- was bubbled with 95% O_2 –5% CO_2 . Both sides were gassed with 100% O_2 during experiments with bilateral HCO_3^- -free solution.

To maintain viability during long fluid secretion experiments, EMEM medium containing essential amino acids was placed on the basolateral side. The salts of amino acids (L-histidine-HCl, L-lysine-HCl) and vitamins (choline chloride, pyridoxine-HCl, thiamine-HCl) contributed 0.6 mmol l^{-1} Cl^- to the nominally Cl^- -free medium. This Cl^- contamination probably did not affect the results since adding this concentration of Cl^- during pH-stat measurements had no detectable effect on I_{eq} , which is a measure of the net $\text{Cl}^- + \text{HCO}_3^-$ flux under open-circuit conditions. Monolayers bathed with basolateral 25 mmol l^{-1} HCO_3^- medium were kept in 5% CO_2 –95% air, which was nominally saturated with H_2O during fluid secretion measurements unless otherwise noted. Control experiments performed with Transwells mounted on an orbital shaker in a 5% CO_2 –95% O_2 atmosphere to allow better oxygenation yielded only slightly higher fluid secretion rates (data not shown). Humidified air (0.035% CO_2) was used when measuring fluid secretion with nominally HCO_3^- -free basolateral medium. Tracer fluxes were measured using the same solutions as during pH-stat experiments (i.e. with a basolateral-to-apical HCO_3^- gradient) except apical pH was maintained using Hepes rather than by titrating with acid. In some experiments the basolateral membrane was permeabilized by adding nystatin from a 1000 \times stock solution in DMSO (final nystatin concentration 100 $\mu\text{g ml}^{-1}$). The CFTR inhibitor GlyH-101 was added from a 1000 \times stock solution to give a final concentration of 100 $\mu\text{mol l}^{-1}$ and 0.1% DMSO.

Immunoblotting

After SDS-PAGE on 8% gels, proteins were transferred to nitrocellulose membranes as described previously (Luo *et al.* 2009) and probed with the following monoclonal antibodies: M3A7, which recognizes an epitope between amino acids 1365 and 1395 in the second nucleotide binding domain of CFTR (1:5000, gift from J.R. Riordan

and T.J. Jensen, UNC Chapel Hill, NC, USA; Kartner & Riordan, 1998), TUB-1A2, which binds to the C-terminus of α -tubulin (1:5000, Sigma) and α 5, which binds the α -subunit of avian Na^+/K^+ -ATPase (1:200, mAb gift from R.W. Mercer, Washington University, St Louis, MO, USA; Takeyasu *et al.* 1988). Blots were washed, incubated with secondary antibody conjugated to horseradish peroxidase (1:1000), visualized by enhanced chemiluminescence (Amersham Biosciences) and analysed using ImageJ (Rasband, 2011).

Measurement of equivalent short-circuit current (I_{eq}) and HCO_3^- secretion

Inserts were mounted in modified Ussing chambers (Physiologic Instruments, Inc., San Diego, CA, USA) at 37°C. Initial studies were carried out under voltage clamp to allow comparison of net HCO_3^- flux with I_{sc} ; however, in all subsequent experiments, net HCO_3^- secretion was measured under open-circuit conditions and compared with I_{eq} , which was calculated from Ohm's law using the spontaneous transepithelial potential (V_t) and resistance (R_t). R_t was determined from the small deflections in V_t produced by bipolar current pulses (1 μA , 1 s duration, 99.9 s interval, duty cycle 100.9 s) delivered by the voltage clamp (VCC200, Physiologic Instruments, Inc.). Data were digitized (Powerlab 8/30, AD Instruments, Montreal, QC, Canada) and analysed using Chart5 software.

HCO_3^- transport was measured using pH-stat under both open- and short-circuit conditions. A mini-pH electrode (pHG200-8, Radiometer Analytical) connected to the automated titration workstation (TitraLab 854, Radiometer) delivered 1 μl aliquots of 10 mmol l^{-1} HCl or 5 mmol l^{-1} H_2SO_4 to maintain the pH constant at 7.400 ± 0.002 . To avoid offsets, the 'metal' option for cell grounding was selected in the Titralab firmware, the pH4000 pH electrode was connected to the E1 input of the titrator, and the current electrode of the voltage clamp in the same half-chamber was connected to the GND input of the Titralab.

The amount of acid required to maintain pH constant was used to calculate the rate of HCO_3^- secretion. The volume of each half chamber was 4 ml. Solutions containing 25 mmol l^{-1} HCO_3^- were stirred vigorously with 95% O_2 -5% CO_2 . Nominally HCO_3^- -free solutions were bubbled with 100% O_2 .

Volume and composition of the secreted fluid

Fluid was aspirated from the apical surface and fresh media containing replacement ions, activators or inhibitors were added on the basolateral side to begin fluid secretion assays. In some experiments, agents were added to the apical side in a small volume of Krebs-Henseleit solution

(mmol l^{-1} : 120 NaCl, 25 NaHCO_3 , 3.3 KH_2PO_4 , 0.8 K_2HPO_4 , 1.2 MgCl_2 , 1.2 CaCl_2 and 10 mannitol), which was subtracted from the volume measured at the end of the experiment when calculating secretion. Apical fluid was collected at 24 h intervals using a pipettor and the time averaged fluid secretion rate was calculated after subtracting the volume of vehicle if added on the apical side. Although cumulative volume increased linearly for at least 3 days, the instantaneous secretion rate declined over the course of each 24 h collection period, therefore total volume secreted under these conditions is sub-maximal. A low rate of evaporation was observed from siliconized Transwells in control measurements ($\sim 0.27 \mu\text{l cm}^{-2} \text{h}^{-1}$) despite being kept in a humidified incubator. However, when cultures were coated with a film of water-saturated hexadecane (a solvent with low vapour pressure which eliminates evaporation), the volume of secreted fluid that could be retrieved from cell monolayers was not altered. High osmotic permeability apparently enables sufficient H_2O diffusion through the monolayer to compensate for evaporative H_2O loss from the surface of uncoated cultures so that apical fluid volume is determined simply by the quantity of solute on the surface. Since correcting for evaporation would cause overestimation of active fluid transport, no correction was applied. The Cl^- concentrations of secretions and media were measured using an ADVIA 1650 biochemistry system (Bayer) after 10-fold dilution in distilled H_2O . pH was measured using a micro-electrode (9826BN, Orion), which was either kept inside the 5% CO_2 incubator to reduce equilibration time or immersed in the sample while bubbling with 5% CO_2 . The Henderson-Hasselbalch equation was used to calculate the equilibrium HCO_3^- concentration:

$$\text{pH} = \text{pK} + \log \left(\frac{[\text{HCO}_3^-]}{P_{\text{CO}_2} \times 0.03} \right) \quad (1)$$

where $\text{pK} = 6.09$ and $P_{\text{CO}_2} = \% \text{CO}_2 / 100 \times (760 - 47)$. No corrections were made for small errors in water vapour pressure (slightly less than 47 mmHg), laboratory elevation above sea level (~ 31 m) or daily fluctuations in barometric pressure. P_{CO_2} in the incubator was set using the built-in infrared controller and confirmed independently within $\pm 0.01\%$ using an external non-dispersive infrared (NDIR) sensor (GMM221, Vaisala, Lake Villa, IL, USA).

Tracer fluxes

Calu-3 monolayers were mounted in modified Ussing chambers and equilibrated for 20 min. H^{36}Cl (generous gift of W.S. Marshall, St Francis-Xavier University, Antigonish, NS, Canada) was added to one side of the monolayer and neutralized, yielding a final Cl^- concentration of 125.3 mmol l^{-1} . Duplicate 400 μl samples were taken from

the cold side after 20 min (to allow mixing), and again at 15 min intervals with replacement by 800 μl saline. Residual radioactivity was calculated (with correction for dilution) at the beginning of each subsequent flux period and samples were counted in 5 ml scintillation solution (Tri-Carb 2810 TR, PerkinElmer, Woodbridge, ON, Canada). Two 10 μl samples taken from the hot side at the beginning and end of each experiment were averaged and used to calculate mean specific activity of the tracer, which ranged between 6500 and 8000 cpm μmol^{-1} . Counts on the cold side at the end of the sample period were several-fold above background. Unidirectional fluxes were measured in parallel experiments at the same time. R_t ranged between 200 and 300 $\Omega\text{ cm}^2$ under resting conditions.

To measure ^{36}Cl fluxes under conditions similar to those when monitoring fluid secretion, monolayers were stimulated with 10 $\mu\text{mol l}^{-1}$ forskolin and $^{36}\text{Cl}^{-}$ was added to basolateral serum-free EMEM medium (2.5 ml) or to apical Krebs–Henseleit solution (400 μl) in Transwells rather than in Ussing chambers. Mean specific activity was determined for each experiment by averaging the number of counts on the hot side at the beginning and end of the 24 h flux period. J_{sm} (serosal-to-mucosal $^{36}\text{Cl}^{-}$ flux), J_{ms} (mucosal-to-serosal $^{36}\text{Cl}^{-}$ flux) and J_{net} (net $^{36}\text{Cl}^{-}$ flux) were calculated by counting 100 μl samples from the cold side, after correction for residual tracer and replacement volume.

Data analysis

Either I_{sc} or I_{eq} was determined at 100 s intervals, and HCO_3^{-} net flux rate was calculated every 5 min. Basal values were those obtained immediately before adding forskolin. Steady-state fluxes during stimulation were calculated 30–60 min after forskolin. Paired or unpaired Student's *t* tests with $P < 0.05$ were used for single comparisons, whereas one-way analysis of variance followed by the Bonferonni *post hoc* test was used for multiple comparisons.

Results

HCO_3^{-} secretion accounts for the short-circuit current (I_{sc})

Electrogenic HCO_3^{-} secretion across control monolayers was measured under voltage-clamp and compared with the I_{sc} measured simultaneously. Unstimulated HCO_3^{-} secretion and I_{sc} were both low but increased ~ 8 -fold after forskolin (10 $\mu\text{mol l}^{-1}$) was added to the basolateral side (Fig. 1). The rate of HCO_3^{-} secretion measured using pH-stat with the transepithelial potential clamped at 0 mV was equal to the I_{sc} within measurement error

(net HCO_3^{-} secretion: $2.14 \pm 0.36 \mu\text{eq cm}^{-2} \text{ h}^{-1}$; I_{sc} : $2.30 \pm 0.27 \mu\text{eq cm}^{-2} \text{ h}^{-1}$; Fig. 1), evidence that basal and forskolin-stimulated I_{sc} were both due to net HCO_3^{-} secretion. This confirms previous suggestions based on the large discrepancy between I_{sc} and the net $^{36}\text{Cl}^{-}$ and $^{22}\text{Na}^{+}$ fluxes (Lee *et al.* 1998; Devor *et al.* 1999), but differs from pH-stat results obtained during 1-EBIO stimulation, when HCO_3^{-} secretion accounted for 70% of the I_{sc} and the discrepancy was due to acid secretion by $\text{H}^{+}/\text{K}^{+}$ -ATPase (Krouse *et al.* 2004). The effects of 1-EBIO were not examined in the present study. The pH-stat technique required unbuffered solution on the apical side and therefore a transepithelial HCO_3^{-} gradient; however, the basolateral-to-apical gradient of 25 mmol l^{-1} HCO_3^{-} did not cause overestimation of HCO_3^{-} secretion since the I_{sc} was not noticeably affected when 25 mol l^{-1} $\text{HCO}_3^{-}/5\% \text{ CO}_2$ was added acutely on the apical side (data not shown), consistent with a previous report (Krouse *et al.* 2004). The stimulated I_{sc} was similar whether symmetrical HCO_3^{-} solutions or pH-stat conditions were used, further evidence that passive diffusion due to the HCO_3^{-} gradient contributed little to I_{sc} .

HCO_3^{-} secretion is CFTR dependent

To evaluate the role of CFTR during HCO_3^{-} and fluid transport, protein expression and anion secretion were compared in control and CFTR knock-down monolayers. The immunoblot in Fig. 2A shows CFTR expression. For comparison, Lanes 1 and 2 show baby hamster kidney (BHK) cells stably transfected with wild-type or ΔF508 -CFTR, Lanes 3 and 4 show parental Calu-3 cells, and Lanes 5 and 6 show shRNA control and CFTR knock-down Calu-3 cells, respectively.

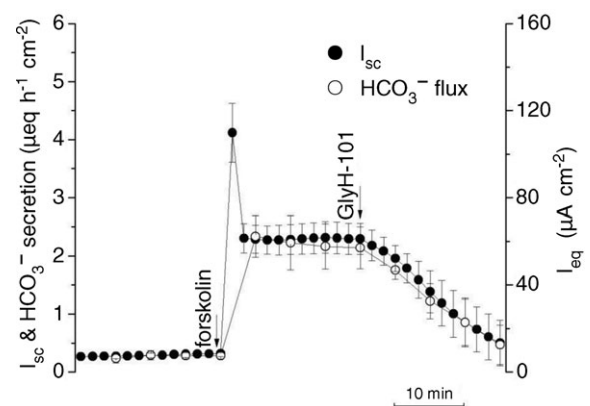


Figure 1. Relationship between short-circuit current (I_{sc}) and HCO_3^{-} secretion

Forskolin (10 $\mu\text{mol l}^{-1}$) and GlyH-101 (100 $\mu\text{mol l}^{-1}$) were added to control Calu-3 cells expressing mutated shRNA. Note the close agreement between I_{sc} and HCO_3^{-} secretion, and their sensitivity to the CFTR channel inhibitor GlyH-101 ($n = 4$). ●, I_{sc} , short-circuit current; ○, HCO_3^{-} secretion as measured using pH-stat.

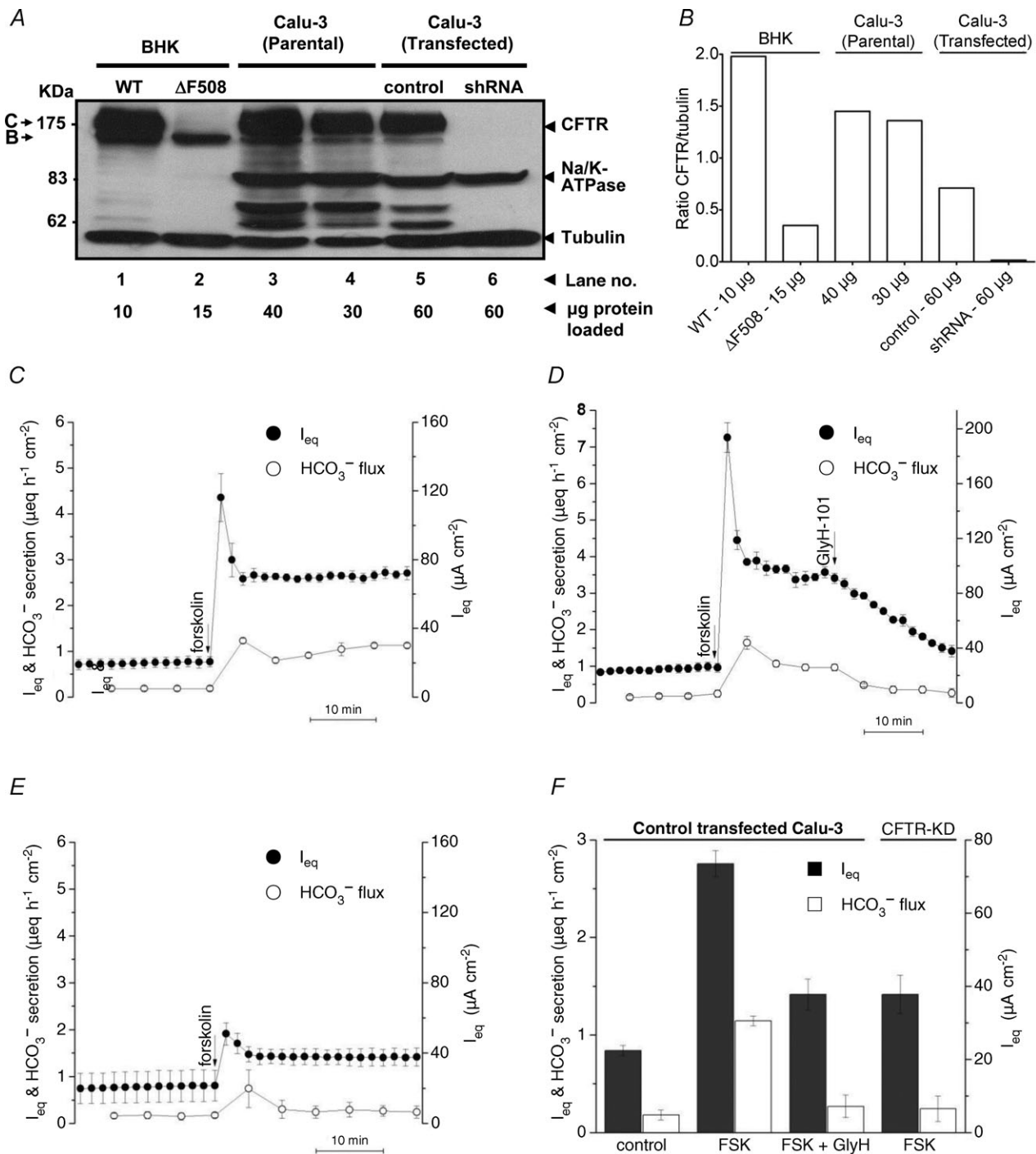


Figure 2. CFTR expression and HCO_3^- secretion

A, CFTR expression in stable cell lines. Lane 1, baby hamster kidney (BHK) cells transfected with wild-type CFTR expressed both mature and immature CFTR. Lane 2, BHK cells transfected with $\Delta F508$ CFTR expressed only immature (band B) CFTR. Lanes 3 and 4, parental, and Lane 5 control transfected Calu-3 cells also expressed both bands B and C. Lane 6, CFTR was not detectable in shRNA knock-down cells. Comparisons of band intensities and μg protein loaded indicate the following relative expression levels: BHK \gg Calu-3 (Parental) $>$ Calu-3 (control transfected) \gg Calu-3 (shRNA transfected). This blot is representative of two experiments. B, mean densities of CFTR normalized to tubulin ($n = 2$). C, forskolin ($10\ \mu mol\ l^{-1}$) stimulated I_{eq} and HCO_3^- secretion across wild-type Calu-3 cells under open-circuit conditions ($n = 12$). D, CFTR inhibitor GlyH-101 ($100\ \mu mol\ l^{-1}$) nearly abolished forskolin-stimulated I_{sc} and HCO_3^- secretion ($n = 6$). E, the forskolin response was greatly reduced in CFTR-knock-down Calu-3 cells ($n = 6$). \bullet , I_{eq} ; \circ , HCO_3^- secretion. F, summary of forskolin-stimulated I_{eq} (filled bars) and HCO_3^- secretion (open bars) shown in C, D and E. Means \pm SEM.

Table 1. Unidirectional ^{36}Cl fluxes across Calu-3 cell monolayers

	J_{sm}	J_{ms}	J_{net}	I_{eq}	R_t	V_t
Control	1.10 ± 0.12	0.53 ± 0.11	0.58 ± 0.06	0.81 ± 0.06	375 ± 47	-8.14 ± 0.68
Forskolin (10 $\mu\text{mol l}^{-1}$)	3.13 ± 0.13***	1.63 ± 0.15***	1.51 ± 0.02***	2.75 ± 0.13***	289 ± 30	-21.31 ± 0.97***
Bumetanide (20 $\mu\text{mol l}^{-1}$)	1.95 ± 0.08+++	1.22 ± 0.06++	0.73 ± 0.05+++	2.15 ± 0.10+++	301 ± 32	-17.35 ± 0.64+++

Experiments were performed under open-circuit, pH-stat conditions (i.e. basolateral 25 mM HCO_3^- , apical 0 mM HCO_3^-). The apical solution was stirred with 100% O_2 and buffered at pH 7.4 using 10 mmol l^{-1} tricine. Forskolin was added to both sides. Bumetanide was added basolaterally. J_{sm} (serosal-to-mucosal $^{36}\text{Cl}^-$ flux), J_{ms} (mucosal-to-serosal $^{36}\text{Cl}^-$ flux), J_{net} (net $^{36}\text{Cl}^-$ flux), I_{eq} (equivalent short-circuit current) have units of $\mu\text{eq cm}^{-2} \text{h}^{-1}$. R_t (transepithelial resistance) has units of Ohms cm^2 electrical resistance, no time units. Values are mean ± SEM, $n = 4$ ($^{36}\text{Cl}^-$ fluxes) or 8 (I_{eq} , R_t and V_t). *** $P < 0.001$, forskolin vs. control; +++ $P < 0.001$; ++ $P < 0.01$, bumetanide vs. forskolin.

BHK cells expressed mature (i.e. complex glycosylated or 'band C' polypeptide) and immature (core-glycosylated, band B) wild-type CFTR, whereas only band B was detected in BHK cells expressing ΔF508 CFTR (Lanes 1 and 2, respectively). Mature and immature CFTR glycoforms were also found in parental cells (Lanes 3 and 4), and in cells expressing control (i.e. altered) shRNA (Lane 5). CFTR was usually not detectable in cells that expressed shRNA targeting CFTR transcripts (Lane 6). Blots were also probed with anti-tubulin antibody to control for variations in protein loading, and with anti- Na^+/K^+ -ATPase antibody to assess non-specific changes in membrane protein expression. Tubulin and Na^+/K^+ -ATPase α subunit levels were not affected by control or CFTR-specific shRNA. Densitometry of CFTR expression revealed >95% reduction in band C compared with the control cell line (Fig. 2B), consistent with previous estimates (Palmer *et al.* 2006). Band C was lower in shRNA control cells than in parental cells after normalization to tubulin, despite the presence of four mutations in the shRNA which were intended to reduce its binding to CFTR mRNA transcripts (Fig. 2B). Cells expressing control shRNA (referred to previously as 'alter' by (Palmer *et al.* 2006) were used as the control cell line in subsequent transport experiments, bearing in mind CFTR expression is lower in these control cells than in parental Calu-3 cells used for previous studies.

The effect of knocking down CFTR expression on HCO_3^- secretion was also investigated under open-circuit conditions using the pH-stat technique (Fig. 2C). In marked contrast to I_{sc} , the I_{eq} calculated from transepithelial voltage and resistance was higher than the simultaneously measured HCO_3^- flux; mean I_{eq} was $2.76 \pm 0.13 \mu\text{eq cm}^{-2} \text{h}^{-1}$ ($n = 12$) during forskolin stimulation whereas net HCO_3^- transport was $1.14 \pm 0.05 \mu\text{eq cm}^{-2} \text{h}^{-1}$ ($n = 12$, Fig. 2F). This difference between I_{eq} and net HCO_3^- flux ($\sim 1.55 \mu\text{eq cm}^{-2} \text{h}^{-1}$) was current carried by Cl^- because, as shown below (Table 1), a net Cl^- flux of $1.5 \mu\text{eq cm}^{-2} \text{h}^{-1}$ in the secretory direction was observed

when unidirectional ^{36}Cl fluxes were measured under these conditions (i.e. open-circuited and with the same 25 mmol l^{-1} HCO_3^- gradient that was present during pH-stat experiments). Also, the discrepancy between I_{eq} and net HCO_3^- flux was abolished in Cl^- -free solution. I_{eq} and net HCO_3^- secretion were both inhibited by the CFTR channel blocker GlyH-101; however, this inhibition developed slowly (100 $\mu\text{mol l}^{-1}$; ~ 20 min, Fig. 1 and 2D; Muanprasat *et al.* 2004), perhaps due to slow diffusion through the hydrophobic mucus gel on the apical surface. Alternatively, GlyH-101 inhibition is voltage dependent therefore its affinity may decline as CFTR channels become progressively blocked and the membrane potential hyperpolarizes. The stimulation of I_{eq} and HCO_3^- secretion by forskolin was greatly reduced in CFTR knock-down cells compared with control cells (compare Fig. 2E and C), although the decrease in CFTR channel function was somewhat less than the decrease in CFTR protein expression observed on immunoblots (65% vs. 95% reduction). Figure 2F summarizes the mean I_{eq} (filled bars) and HCO_3^- flux (open bars) across control vs. CFTR-deficient cells. HCO_3^- was secreted by CFTR knock-down cells during forskolin stimulation at a rate that was similar to unstimulated control monolayers, and to stimulated control monolayers treated with the CFTR inhibitor GlyH-101. Taken together the results confirm that forskolin stimulates electrogenic HCO_3^- secretion and are consistent with CFTR channels mediating part of this flux.

The stimulated I_{eq} under open-circuit, pH-stat conditions in Fig. 2C was $2.55 \mu\text{eq cm}^{-2} \text{h}^{-1}$, higher than the HCO_3^- flux of $1.0 \mu\text{eq cm}^{-2} \text{h}^{-1}$ measured simultaneously. To examine if the discrepancy of $\sim 1.55 \mu\text{eq cm}^{-2} \text{h}^{-1}$ is carried by Cl^- , unidirectional $^{36}\text{Cl}^-$ tracer fluxes were measured under the same conditions, i.e. open circuited and with a basolateral \rightarrow apical HCO_3^- gradient and apical O_2 bubbling. Apical pH was maintained by 25 mM Hepes during tracer experiments rather than by titration with acid. As shown in Table 1, net Cl^- secretion (J_{net}) was observed under basal conditions. Forskolin increased $^{36}\text{Cl}^-$ fluxes in both

directions, but stimulation of the secretory flow was larger and resulted in a 3-fold increase in the net flux. Thus, Cl^- was secreted under open circuit/pH-stat conditions (in marked contrast to I_{sc} conditions), and the net flux rate ($1.51 \pm 0.02 \mu\text{eq cm}^{-2} \text{h}^{-1}$) accounted for the discrepancy of $1.55 \mu\text{eq cm}^{-2} \text{h}^{-1}$ between I_{eq} and net HCO_3^- flux measured using the pH-stat.

Proton secretion neutralizes some of the transported bicarbonate

Acid secretion was also investigated because, if present, it could cause underestimation of the HCO_3^- flux. Air-

way epithelial cells secrete H^+ by multiple mechanisms (Acevedo & Steele, 1993; Fischer *et al.* 2002; Coakley *et al.* 2003; Inglis *et al.* 2003), two of which are electrically silent (H^+/K^+ -ATPase and Na^+/H^+ exchange) and thus capable of increasing the discrepancy between I_{eq} and HCO_3^- secretion. The other two mechanisms (electrogenic vacuolar H^+ -ATPase and H^+ channels) would be invisible in these experiments because they would cause equivalent reductions in current and net HCO_3^- flux.

To assess the role of the non-gastric isoform of H^+/K^+ -ATPase, the effect of apical ouabain on I_{eq} and HCO_3^- secretion was investigated (Fig. 3A).

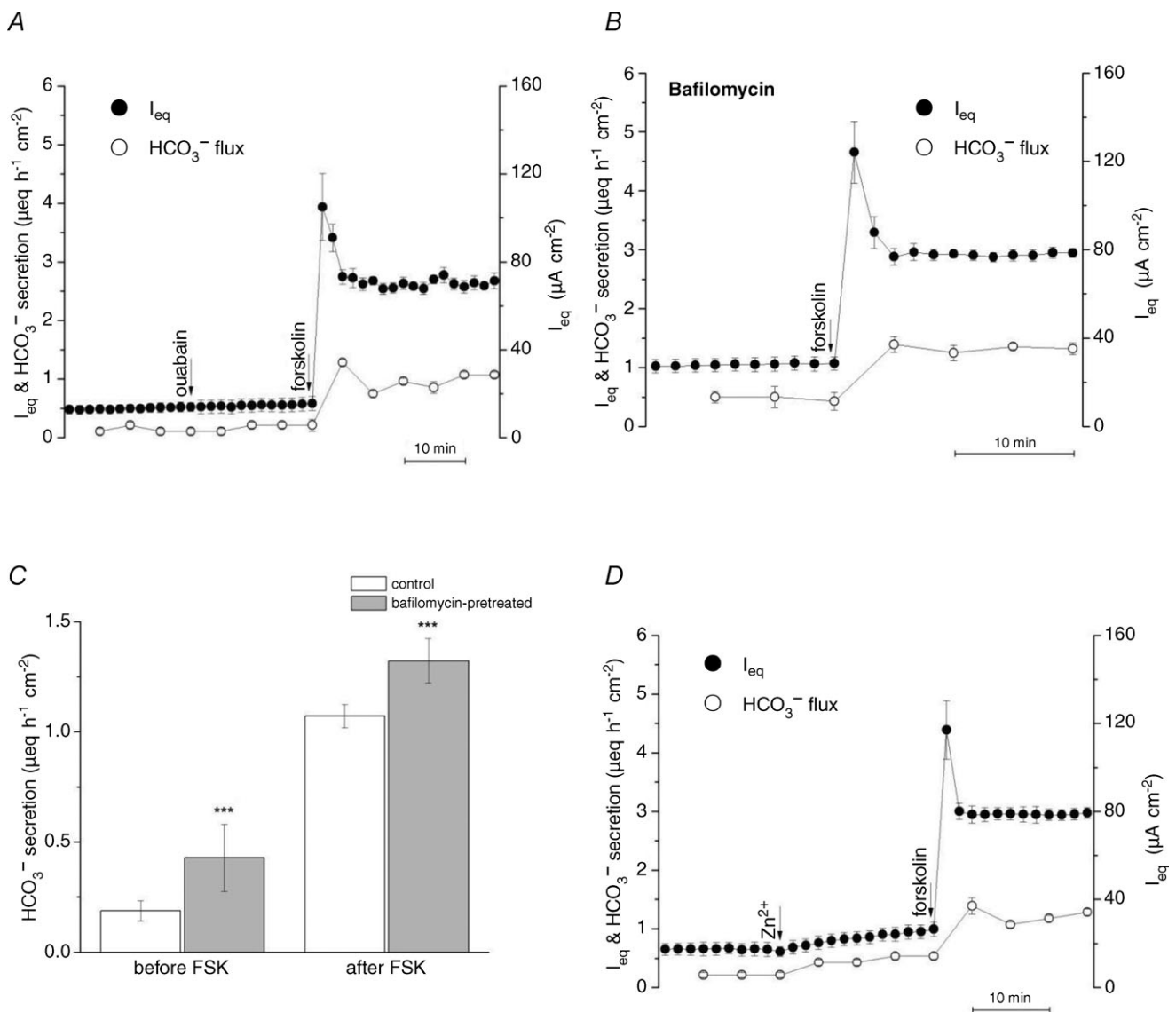


Figure 3. Effect of proton transport inhibitors on I_{eq} and net HCO_3^- secretion across Calu-3 'Alter' shRNA control cells

A, ouabain ($100 \mu\text{mol l}^{-1}$) had no effect when added to the apical side to inhibit putative H^+/K^+ -ATPase ($n = 3$), B and C, pretreatment with the V-ATPase inhibitor bafilomycin (50nmol l^{-1}), increased basal- and forskolin-stimulated HCO_3^- secretion ($n = 3$). D, apical addition of ZnCl_2 (nominally 1mmol l^{-1}) to block putative H^+ channels increased I_{eq} and HCO_3^- secretion ($n = 3$). ●, I_{eq} ; ○, HCO_3^- secretion. *** $P < 0.001$.

Ouabain ($100 \mu\text{mol l}^{-1}$) did not alter basal or forskolin-stimulated I_{eq} or HCO_3^- secretion, suggesting little role of ouabain-sensitive H^+/K^+ -ATPase activity with an apical solution containing $5 \text{ mmol l}^{-1} \text{ K}^+$ and bubbled with 100% O_2 . Apical amiloride (1 mmol l^{-1}) also had no effect (data not shown), evidence against significant apical proton secretion via Na^+/H^+ exchange under these conditions. By contrast, pretreating cells with the vacuolar H^+ -ATPase inhibitor bafilomycin for 30 min increased I_{eq} and HCO_3^- secretion by $\sim 0.25 \mu\text{eq cm}^{-2} \text{ h}^{-1}$, and similar increases were obtained under basal and forskolin-stimulated conditions (Fig. 3B and C). This implies that forskolin did not cause insertion of additional proton pumps into the apical membrane (Paunescu *et al.* 2010). Finally, acute exposure to ZnCl_2 (1 mmol l^{-1}), which inhibits acid secretion by blocking apical H^+ (HVCN1) channels in airway epithelial cells (Iovannisci *et al.* 2010), increased I_{sc} and HCO_3^- secretion by $\sim 0.25 \mu\text{eq cm}^{-2} \text{ h}^{-1}$ (Fig. 3D), implicating proton channels in H^+ efflux. Taken together these inhibitor studies indicate that HCO_3^- secretion is 30% higher across Calu-3 monolayers than the measured net flux, but is partially neutralized by parallel H^+ secretion. These electrogenic H^+ transport mechanisms would not cause any discrepancy between I_{eq} and HCO_3^- net flux and are thus compatible with the close agreement between the unidentified I_{eq} and $^{36}\text{Cl}^-$ net flux and the net HCO_3^- flux and I_{sc} under voltage clamp.

Fluid secretion is CFTR dependent

Dehydration is a hallmark of CF airway secretions, and suggests a role of CFTR in fluid secretion. To test if fluid transport by Calu-3 cells is CFTR dependent, apical fluid was removed at time 0 h and secretions were collected from control and CFTR knock-down cultures at 24 h intervals under control conditions and during forskolin stimulation (Fig. 4A). Little fluid was produced by control monolayers that were left untreated or exposed only to vehicle (0.1% basolateral DMSO). However, fluid secretion increased to $>40 \mu\text{l day}^{-1}$ during stimulation with forskolin ($10 \mu\text{mol l}^{-1}$), and a similar volume was produced for several days, leading to the cumulative secretion of $\sim 130 \mu\text{l}$.

Figure 4B shows the time-averaged fluid secretion rate measured daily for 3 days under each condition. GlyH-101 ($100 \mu\text{mol l}^{-1}$) nearly abolished forskolin-stimulated fluid secretion when added to the apical side in $400 \mu\text{l}$ PBS, suggesting CFTR channel activity is required for fluid transport.

CFTR mediates apical HCO_3^- conductance

The next series of experiments used control and CFTR knock-down Calu-3 cells to examine whether CFTR

can directly mediate HCO_3^- flux. Monolayers were voltage-clamped at 0 mV, the basolateral membrane was permeabilized using nystatin ($360 \mu\text{g ml}^{-1}$), and an apical \rightarrow basolateral gradient of 25 mM HCO_3^- was imposed. Adding forskolin to control monolayers under these conditions caused a rapid (i.e. negative) I_{sc} , which was blocked by the inhibitor $\text{CFTR}_{\text{inh}}-172$ ($10 \mu\text{mol l}^{-1}$; Ma *et al.* 2002), suggesting ion diffusion through CFTR channels (Gray *et al.* 1990; Poulsen *et al.* 1994; Linsdell *et al.* 1997; Illek *et al.* 1997) (Fig. 5A).

Forskolin did not stimulate I_{sc} across CFTR knock-down cells under these conditions (Fig. 5A). Figure 5B shows the mean I_{sc} measured across basolaterally permeabilized monolayers. Although these results do not exclude other apical exit mechanisms, they do show that forskolin-stimulated I_{sc} is $\text{CFTR}_{\text{inh}}-172$ -sensitive and reduced by 88% in CFTR knock-down cells, consistent with the decrease in CFTR protein expression. The

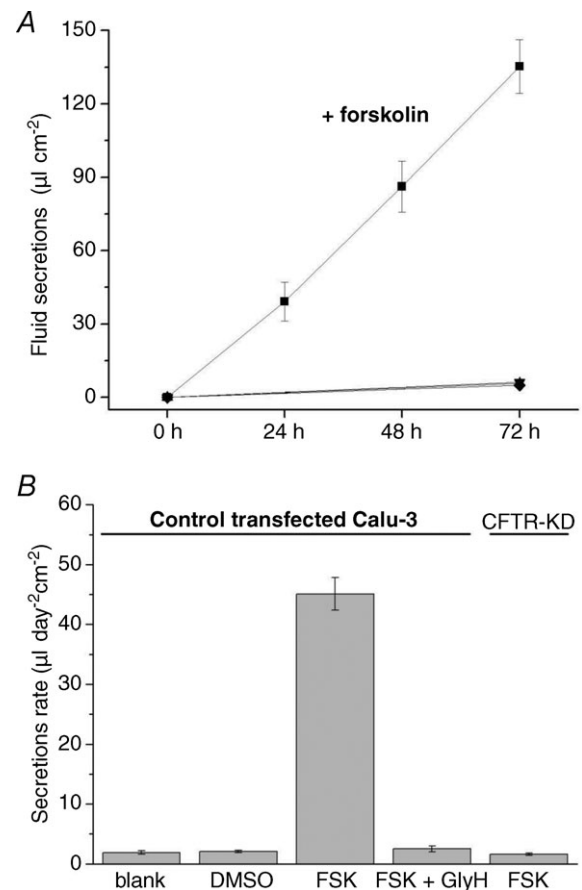


Figure 4. CFTR-dependent fluid secretion by control and CFTR knock-down Calu-3 cells

A, fluid secretion under different conditions: ■, control Calu-3 cells stimulated by $10 \mu\text{mol l}^{-1}$ forskolin; ▲, untreated; ▼, 0.1% DMSO or ●, forskolin + GlyH-101 ($100 \mu\text{mol l}^{-1}$)-treated control Calu-3 cells; and ◆, CFTR knock-down Calu-3 cells treated with forskolin ($n = 6$ each condition). B, summary of results in A. Means \pm SEM.

simplest interpretation is that CFTR channels can conduct HCO_3^- and mediate electrogenic HCO_3^- secretion at the apical membrane under these conditions.

Electrogenic anion transport (I_{eq}) requires Na^+ and $\text{CO}_2/\text{HCO}_3^-$

To examine the ionic requirements of HCO_3^- transport under open-circuit conditions, I_{eq} and the appearance of HCO_3^- on the apical side were measured after bilateral removal of $\text{CO}_2/\text{HCO}_3^-$, Na^+ or Cl^- (Fig. 6A–D). The basal and forskolin-stimulated I_{eq} were both abolished in nominally $\text{CO}_2/\text{HCO}_3^-$ -free solution (Fig. 6B).

This dependence of I_{eq} on $\text{CO}_2/\text{HCO}_3^-$ is consistent with Na^+ -n HCO_3^- (NBC)-mediated cotransport at the

basolateral membrane (Devor *et al.* 1999), but also with H_2CO_3 synthesis and subsequent Na^+/H^+ exchange (Cuthbert *et al.* 2003). Forskolin had little effect on I_{eq} under nominally Na^+ -free conditions but did induce electrically silent HCO_3^- secretion of $>0.5 \mu\text{eq cm}^{-2} \text{h}^{-1}$ in the absence of sodium (Fig. 6C). Importantly, transepithelial HCO_3^- transport during forskolin stimulation was 25% higher under bilateral Cl^- -free conditions than when Cl^- was present, despite a 50% reduction in I_{eq} (from 2.76 ± 0.13 to $1.35 \pm 0.32 \mu\text{eq cm}^{-2} \text{h}^{-1}$; compare mean values indicated by open circles in Fig. 6A and E). This argues strongly against $\text{Cl}^-/\text{HCO}_3^-$ exchange as the mechanism of apical HCO_3^- exit under these conditions. I_{eq} was identical to net HCO_3^- secretion under symmetrical Cl^- -free conditions (1.32 ± 0.31 vs. $1.32 \pm 0.19 \mu\text{eq cm}^{-2} \text{h}^{-1}$, respectively), providing further evidence that HCO_3^- -independent I_{eq} measured in control solutions is carried by Cl^- . The large transient I_{eq} normally observed immediately after forskolin addition (e.g. Fig. 6A) was eliminated under bilateral Cl^- -free conditions and therefore may reflect Cl^- and K^+ redistribution when CFTR channels are activated. When Cl^- was removed only from the apical side to generate a favourable Cl^- gradient, forskolin caused more robust stimulation of I_{eq} and a larger discrepancy between I_{eq} and HCO_3^- flux consistent with an increased Cl^- flux (Fig. 6E).

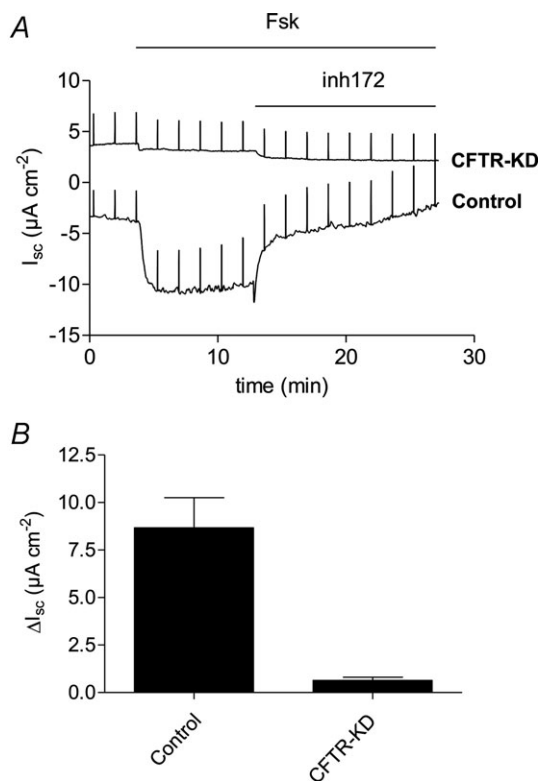


Figure 5. CFTR-dependent HCO_3^- conductance at the apical membrane of permeabilized control and CFTR knock-down (CFTR-KD) Calu-3 monolayers

The basolateral membrane was permeabilized using nystatin and an apical-to-basolateral HCO_3^- gradient $25 \rightarrow 0 \text{ mmol l}^{-1}$ was imposed across the monolayer. A, forskolin (Fsk, $10 \mu\text{mol l}^{-1}$) stimulated a large inward current of $\sim 8 \mu\text{eq cm}^{-2} \text{h}^{-1}$. Forskolin-stimulated inward current in control cells was abolished by the CFTR inhibitor CFTR_{inh}-172 (inh172). Forskolin and CFTR_{inh}-172 had little effect on CFTR-KD monolayers. B, summary of short-circuit currents measured across control ($n = 2$) and CFTR-KD ($n = 3$) cells in the presence of a bicarbonate gradient. Forskolin-stimulated secretion (ΔI_{sc}) was almost abolished in CFTR-KD cells. Means \pm SEM, $P < 0.01$.

Cl^- is the predominant anion in Calu-3 secretions

If net HCO_3^- secretion accounts for I_{sc} and is mediated by the sodium–bicarbonate cotransporter NBCe1 and CFTR, why does fluid secretion depend on Cl^- ? To investigate this, the pH of apical fluid on control (*alter*) and CFTR knock-down monolayers was measured. Surprisingly, the pH of the fluid was in the range 7.2–7.6 when equilibrated with 5% CO_2 (Table 2).

The Cl^- concentration in fluid secreted by control shRNA transfected, CFTR knock-down and parental Calu-3 cell lines was $\sim 120 \text{ mmol l}^{-1}$. Thus, Cl^- was the predominant anion and was 2- to 4-fold higher than the $[\text{HCO}_3^-]$ calculated using the Henderson–Hasselbalch equation. $[\text{HCO}_3^-]$ was similar in secretions collected after several hours or several days of forskolin stimulation (data not shown), and the osmotic pressure of secretions at the end of collection periods was equal to that of the basolateral medium within measurement error (Table 2). Somewhat higher pH (7.7) and HCO_3^- levels (50 mmol l^{-1}) were obtained using parental Calu-3 cells (Table 2), presumably due to their higher CFTR expression; nevertheless, even they produced Cl^- -rich secretions, suggesting most fluid is osmotically driven by transepithelial Cl^- rather than by HCO_3^- secretion despite the close correspondence between I_{sc} and

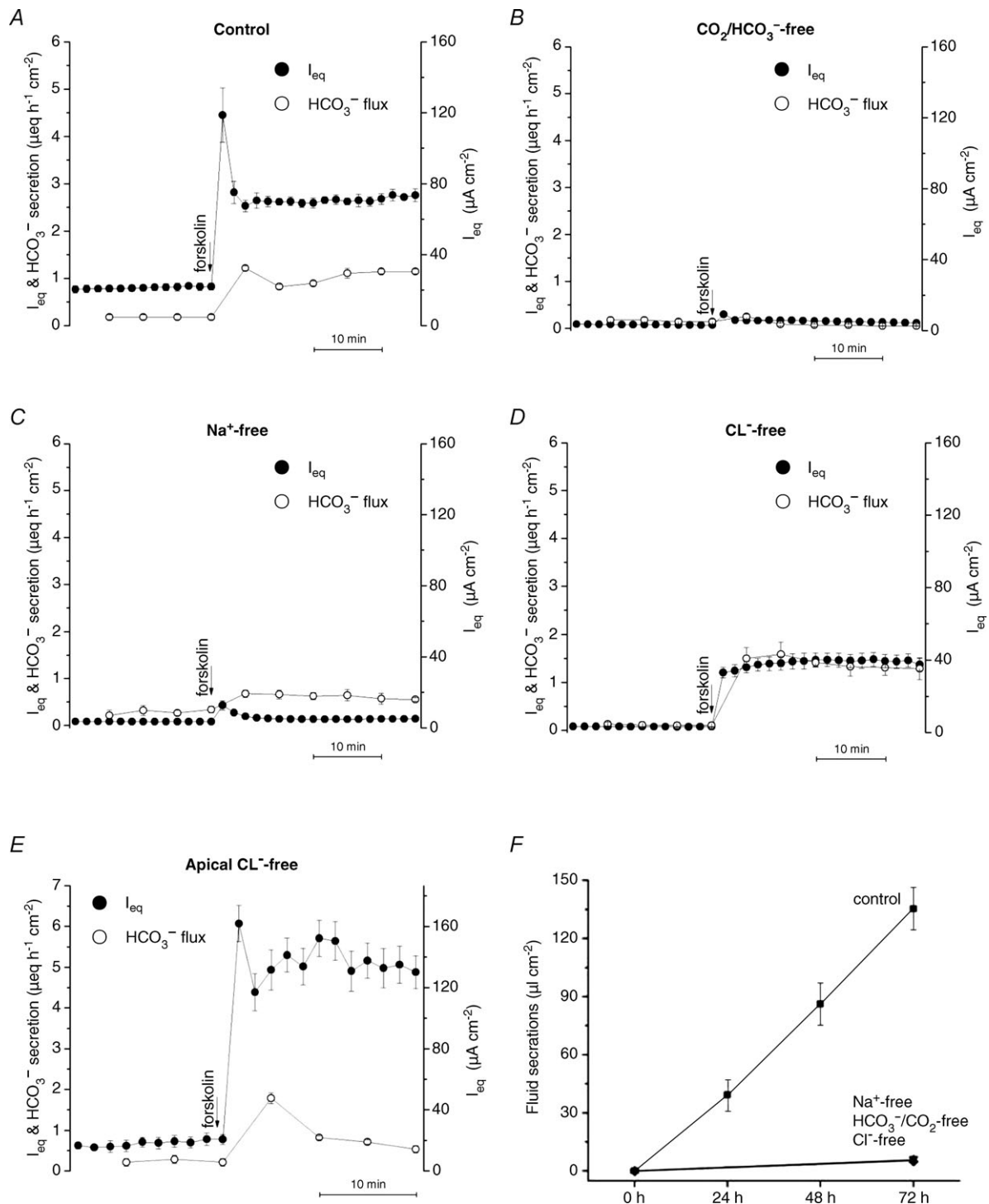


Figure 6. Effects of ion substitutions on anion and fluid transport
 A, the response of Calu-3 'Alter' shRNA control cells to $10 \mu mol l^{-1}$ forskolin in control solutions ($n = 3$). B–D, effect of $10 \mu mol l^{-1}$ forskolin on Calu-3 cells bathed bilaterally with solutions lacking HCO_3^-/CO_2 , Na^+ or Cl^- , respectively ($n = 6$ for each). Forskolin-stimulated HCO_3^- secretion was abolished in the nominal absence of HCO_3^- or Na^+ , but was increased $\sim 25\%$ in Cl^- -free conditions. E, monolayers were bathed with apical Cl^- -free solution, then stimulated with $10 \mu mol l^{-1}$ forskolin. Panels A–E: \bullet , I_{eq} ; \circ , HCO_3^- secretion. F, forskolin-stimulated fluid transport was abolished in the nominal absence of Na^+ , HCO_3^-/CO_2 or Cl^- . \blacksquare , normal medium; \blacktriangle , Na^+ -free medium; \blacktriangledown , Cl^- -free medium; \blacklozenge , HCO_3^-/CO_2 -free medium ($n = 6$ each condition; means \pm SEM).

Table 2. Composition of fluid secreted by Calu-3 monolayers

	Control transfected	CFTR knock-down	Initial medium
Measured [Cl ⁻] (mmol l ⁻¹)	120 ± 5	123 ± 6	135 ± 16
Measured pH	7.55 ± 0.04	7.28 ± 0.02	7.43 ± 0.03
Calculated [HCO ₃ ⁻] (mmol l ⁻¹)	31.35 ± 2.1	16.08 ± 0.52***	24.4 ± 2.2
Osmotic pressure (mosmol l ⁻¹)	309 ± 16	301 ± 6	310 ± 16

Fluid was collected daily during forskolin (10 μmol l⁻¹) stimulation and pooled for analysis. Values are mean ± SEM, *n* = 3–12 each condition. ****P* < 0.001 comparing CFTR knock-down vs. control transfected.

Table 3. Unidirectional ³⁶Cl fluxes across Calu-3 cells under open-circuit conditions

	<i>J</i> _{sm}	<i>J</i> _{ms}	<i>J</i> _{net}	<i>I</i> _{eq}	<i>R</i> _T	<i>V</i> _T
Control	0.73 ± 0.22	0.60 ± 0.19	0.13 ± 0.23	1.05 ± 0.16	344 ± 29	-9.77 ± 0.35
Forskolin (10 μmol l ⁻¹)	1.62 ± 0.21***	1.57 ± 0.25***	0.05 ± 0.14	2.85 ± 0.19***	276 ± 20***	-21.09 ± 0.70***

Experiments were performed in Ussing chambers with symmetrical Cl⁻ and HCO₃⁻ concentrations. Forskolin was added to both sides. *J*_{sm}, *J*_{ms}, *J*_{net}, *I*_{eq}: μeq cm⁻² h⁻¹; *R*_T: ohms cm² h⁻¹ (see Table 1). Values are mean ± SEM, *n* = 6. ****P* < 0.001, forskolin vs. control.

HCO₃⁻ secretion (Fig. 1), and the absence of detectable ³⁶Cl⁻ net flux under *I*_{sc} conditions (Devor *et al.* 1999).

The net Cl⁻ flux needed to account for fluid transport at the observed rate of fluid secretion and [Cl⁻] of the secretions shown in Table 3 was estimated to be small; nevertheless, we attempted to measure it in Ussing chambers under open-circuit conditions.

It was not possible to detect a significant difference between the large unidirectional ³⁶Cl⁻ fluxes (Table 3). Since forskolin caused a modest elevation of apical [HCO₃⁻] (see Table 2, control transfected), unidirectional ³⁶Cl⁻ fluxes were also measured when apical [HCO₃⁻] was increased to 30 and 50 mmol l⁻¹ (Table 4). Net Cl⁻ flux was observed with asymmetrical [HCO₃⁻], although it only reached statistical significance in the experiments with 30 mmol l⁻¹ HCO₃⁻. A more striking effect of exposing forskolin-stimulated monolayers to apical 50 mmol l⁻¹ [HCO₃⁻] was a ~2-fold increase in both unidirectional Cl⁻ fluxes (*P* < 0.01).

HCO₃⁻, Na⁺ and Cl⁻ are all required for forskolin-stimulated fluid secretion

The low [HCO₃⁻] and high [Cl⁻] of Calu-3 secretions prompted us to study the ionic requirements for fluid secretion and *I*_{eq}. Fluid transport was reduced from 45.1 ± 7.9 μl cm⁻² day⁻¹ to 0.8 ± 0.4 μl cm⁻² day⁻¹ when monolayers were bathed with nominally HCO₃⁻-free/low *P*_{CO₂} medium (Fig. 6F), and a similar decrease to 1.0 ± 0.8 μl cm⁻² day⁻¹ was observed in nominally Na⁺-free medium. These effects of removing HCO₃⁻ and Na⁺ were anticipated since *I*_{eq} also depends on these ions (e.g. Fig. 6B and C). More surprising was the effect of replacing Cl⁻ with gluconate, which nearly abolished fluid secretion (from 45.1 ± 7.9 μl cm⁻² day⁻¹ to 2.0 ± 0.7 μl cm⁻² day⁻¹; Fig. 6F). This contrasts with the effect on *I*_{eq}, 60% of which persisted in nominally Cl⁻-free solution (Fig. 6D). Thus, forskolin-stimulated HCO₃⁻ secretion depends on the simultaneous presence of Na⁺ and HCO₃⁻ but not Cl⁻, whereas fluid secretion requires all three ions (Fig. 6F).

Table 4. Effect of apical HCO₃⁻ on unidirectional ³⁶Cl⁻ fluxes across Calu-3 cells under open-circuit conditions

	<i>J</i> _{sm}	<i>J</i> _{ms}	<i>J</i> _{net}	<i>I</i> _{eq}	<i>R</i> _T	<i>V</i> _T
Control 25 HCO ₃ ⁻	0.85 ± 0.10	0.77 ± 0.16	0.08 ± 0.10	0.78 ± 0.11	364 ± 23	-7.61 ± 0.61
Forskolin 25 HCO ₃ ⁻	1.75 ± 0.18***	1.60 ± 0.18***	0.15 ± 0.17	2.70 ± 0.14***	266 ± 14***	-19.26 ± 0.63***
Forskolin 30 HCO ₃ ⁻	1.53 ± 0.12 ⁺⁺	1.27 ± 0.10 ⁺⁺⁺	0.25 ± 0.11 ⁺⁺	2.71 ± 0.12	262 ± 16	-19.03 ± 0.74
Forskolin 50 HCO ₃ ⁻	2.77 ± 0.15 ^{†††}	2.50 ± 0.10 ^{†††}	0.27 ± 0.13	2.75 ± 0.14	254 ± 20	-18.73 ± 0.56

Monolayers were bathed with symmetrical 25 m HCO₃⁻, then with 30 or 50 mmol l⁻¹ HCO₃⁻ on the apical side; 10 μmol l⁻¹ forskolin was added to both sides. *J*_{sm}, *J*_{ms}, *J*_{net}, *I*_{eq}: μeq cm⁻² h⁻¹; *R*_T: ohms cm² h⁻¹. Values are mean ± SEM. ****P* < 0.001, forskolin (25 HCO₃⁻) vs. control. ++, +, *P* < 0.01, *P* < 0.001, forskolin (30 HCO₃⁻) vs. forskolin (25 HCO₃⁻). †††*P* < 0.001, forskolin (50 HCO₃⁻) vs. forskolin (30 HCO₃⁻), control and forskolin (25 HCO₃⁻) (*n* = 8 each) and forskolin (30 HCO₃⁻) and forskolin (50 HCO₃⁻) (*n* = 4 each).

Ion substitution effects and the high $[\text{Cl}^-]$ of secretions suggested that most fluid is osmotically driven by transepithelial Cl^- rather than HCO_3^- transport. Inhibitor studies in the next section examine the role of NKCC1 cotransport and basolateral anion exchange in basolateral Cl^- loading.

Some basolateral Cl^- entry is independent of NKCC

Previous studies of NKCC1's contribution to anion secretion by Calu-3 cells have yielded varying results, perhaps due to different experimental conditions. In the present work, the effect of bumetanide on I_{sc} was measured and compared with its effects on I_{eq} , net HCO_3^- flux, tracer fluxes, and fluid transport under open-circuit conditions. Basolateral bumetanide ($20\text{--}50\ \mu\text{mol l}^{-1}$) did not affect I_{sc} during stimulation by forskolin (data not shown), in good agreement with a previous study (Devor *et al.* 1999). However, under open-circuit conditions bumetanide ($20\ \mu\text{mol l}^{-1}$) inhibited $\sim 20\%$ of the basal (Fig. 7A) and forskolin-stimulated (Fig. 7B) I_{eq} , which monitors both Cl^- and HCO_3^- transport. Bumetanide inhibition of the I_{eq} component carried by Cl^- was $\sim 35\%$ in control-transfected Calu-3 cells (Fig. 7A and B), similar to the results with parental cells (Huang *et al.* 2011) and partial inhibition of I_{sc} noted previously during stimulation by the hyperpolarizing secretagogues 1-EBIO and thapsigargin (Lee *et al.* 1998; Krouse *et al.* 2004).

Net ^{36}Cl flux under these conditions confirmed the bumetanide-sensitive component of I_{eq} was mediated by Cl^- transport (see Table 1) and confirmed that a fraction of the transepithelial Cl^- transport is mediated by NKCC1 when the basolateral membrane is hyperpolarized, either by current flowing through paracellular and transcellular shunt pathways under open-circuit conditions (loop current), or by activation of Ca^{2+} -activated potassium channels under short-circuit conditions. Bumetanide ($20\ \mu\text{mol l}^{-1}$) reduced fluid secretion from 33.5 ± 6.98 to $26.6 \pm 1.39\ \mu\text{l cm}^{-2}\ \text{day}^{-1}$; however, the other 70–80% of the fluid secretion was insensitive to this inhibitor despite the high $[\text{Cl}^-]$ of the secreted fluid (Fig. 7C). Inhibition of fluid transport was not further increased by raising bumetanide concentration to $50\ \mu\text{mol l}^{-1}$ (data not shown). Partial inhibition of fluid transport by bumetanide paralleled its effect on Cl^- -dependent I_{eq} in Ussing chambers, reinforcing the conclusion that substantial Cl^- and fluid transport is independent of NKCC1.

Evidence for basolateral Cl^- loading by anion exchange

To examine if HCO_3^- efflux through basolateral anion exchangers could serve as an alternative Cl^- entry mechanism during anion and fluid secretion, experiments were designed to monitor the 'trans' effect of anions on

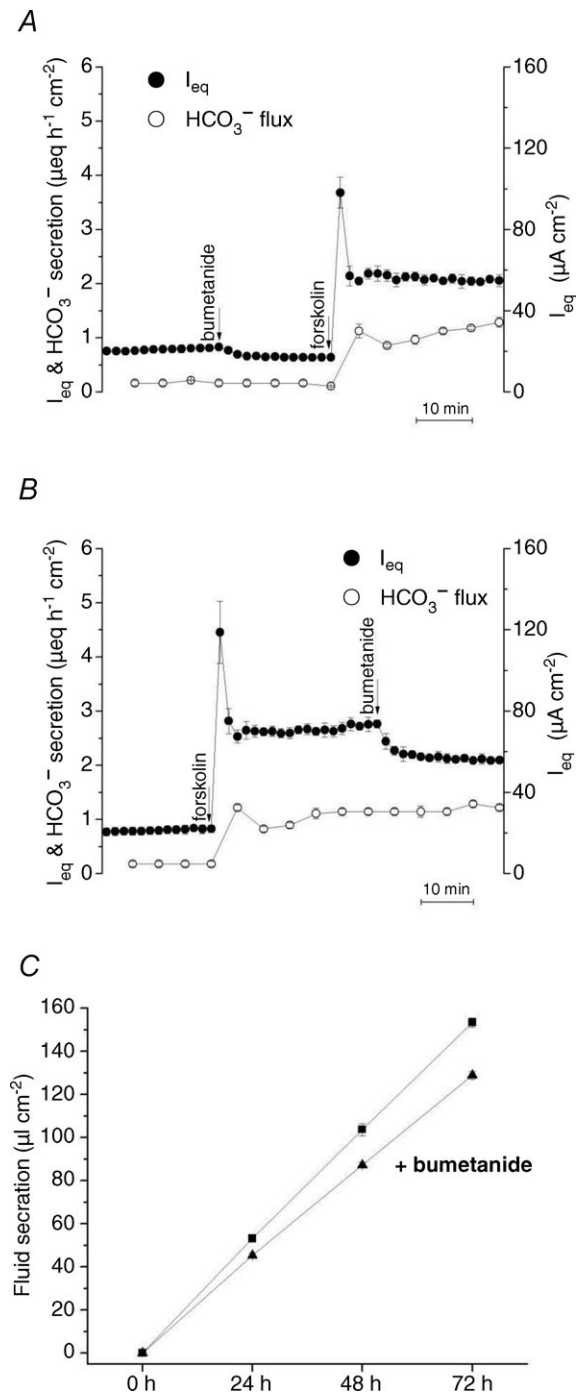


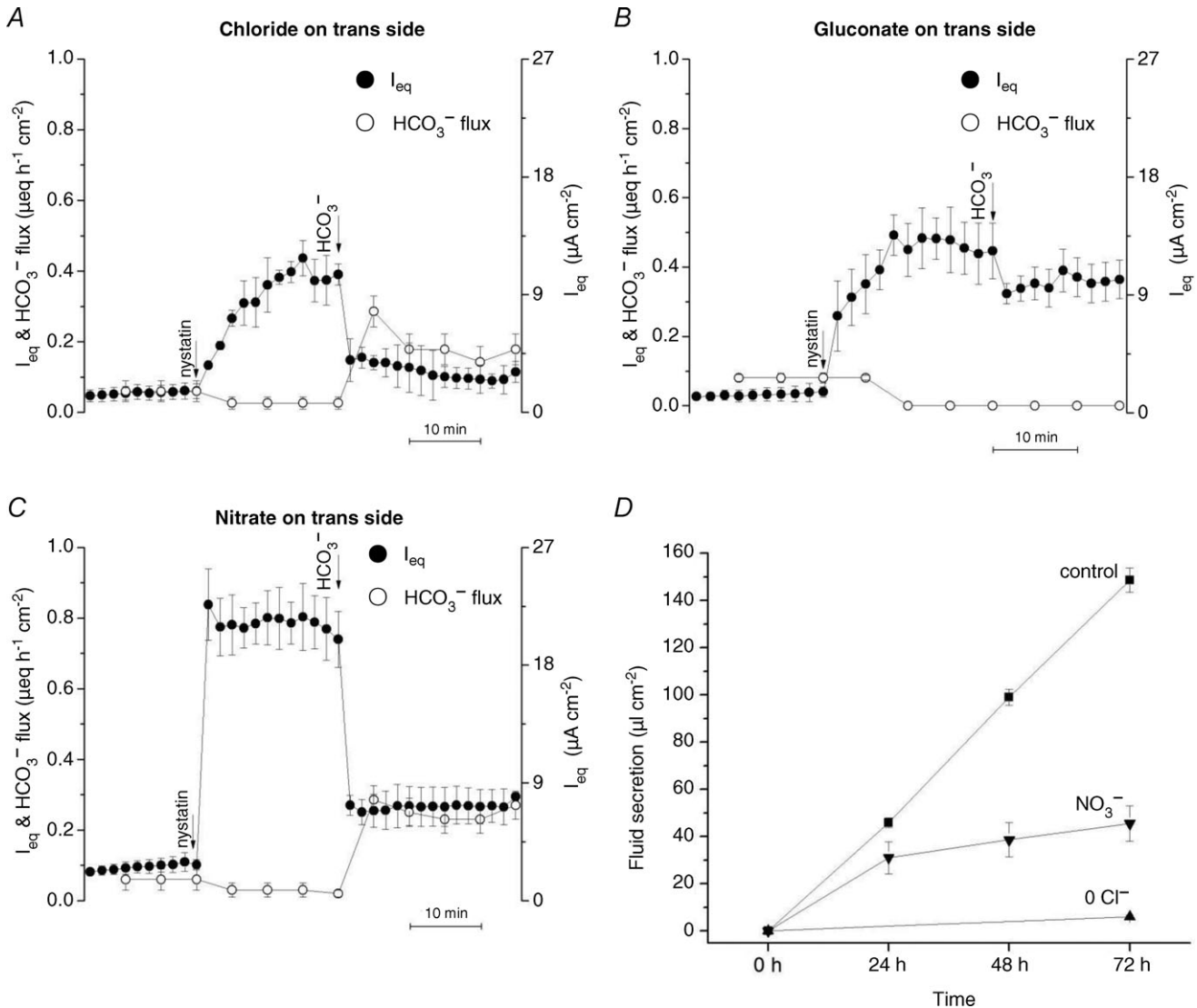
Figure 7. Effects of bumetanide on forskolin-stimulated I_{eq} and fluid secretion

A, basolateral pretreatment with the NKCC1 inhibitor bumetanide ($20\ \mu\text{mol l}^{-1}$) partially inhibited basal I_{eq} ($\sim 20\%$) but did not prevent forskolin-stimulated I_{eq} or HCO_3^- secretion ($n = 6$). B, basolateral bumetanide ($20\ \mu\text{mol l}^{-1}$) inhibited $\sim 20\%$ of the I_{eq} (\bullet) without affecting HCO_3^- secretion (\circ) ($n = 6$). C, forskolin-stimulated fluid secretion was inhibited $\sim 15\%$ by bumetanide (\blacktriangle) when compared with forskolin alone (\blacksquare) ($n = 6$ each condition; means \pm SEM).

the flow of HCO_3^- through the basolateral membrane (Fig. 8). The apical membrane was permeabilized using nystatin ($100 \mu\text{g ml}^{-1}$) while monolayers were bathed with symmetrical HCO_3^- -free solution. After the current reached a plateau, 25 mmol l^{-1} NaHCO_3 was added on the apical side to generate an apical \rightarrow basolateral HCO_3^- gradient and pH-stat was used to monitor the appearance of HCO_3^- on the basolateral side.

As shown in Fig. 8A, apical nystatin induced a large current that was apparently due to electrogenic Na^+ absorption since it was inhibited by basolateral ouabain in control experiments (data not shown) as has been reported for other epithelia (Lewis *et al.* 1978).

After Na^+ current had stabilized, imposing a trans-epithelial HCO_3^- gradient with Cl^- solution bathing the basolateral (trans) side caused I_{eq} to decrease and HCO_3^-



to appear in the basolateral compartment (Fig. 8A). When the same experiment was performed with gluconate solution on the basolateral (trans) side, no HCO_3^- flux to the basolateral side was detected by pH-stat (Fig. 8B). However, robust HCO_3^- flux was produced with basolateral (trans) NO_3^- solution (Fig. 8C). No osmotically induced changes in I_{eq} or HCO_3^- flux were observed in control experiments when 50 mmol l^{-1} mannitol was added instead of 25 mmol l^{-1} NaHCO_3 (Supplementary Fig. S1). These results indicate HCO_3^- flow through the basolateral membrane depends on the nature of the *trans*-anion and are consistent with the activity of basolateral anion exchangers that carry HCO_3^- , Cl^- or NO_3^- but not gluconate ions.

Since NO_3^- substituted for Cl^- during basolateral anion exchange, we wondered if it could also support fluid transport. Forskolin stimulated robust fluid secretion when monolayers were bathed with nominally Cl^- -free NO_3^- medium on the basolateral side (Fig. 8D). The rate of fluid transport from basolateral NO_3^- solution was $>60\%$ of that measured with Cl^- solution during the first 24 h stimulation, then gradually declined, presumably because Cl^- is needed for other cellular processes to maintain viability. Nevertheless, NO_3^- did sustain fluid secretion for many hours, evidence that its basolateral entry is supported by HCO_3^- efflux in permeabilized monolayers. HCO_3^- recycling through basolateral anion exchangers could load Calu-3 cells with either Cl^- or NO_3^- , and both these anions are permeant through apical CFTR channels (Linsdell *et al.* 1997).

Electrogenic HCO_3^- secretion requires carbonic anhydrase

To study the role of HCO_3^- synthesis in anion and fluid secretion, the effects of acetazolamide ($100 \mu\text{mol l}^{-1}$) on I_{eq} and HCO_3^- transport were assayed in Ussing chambers under pH-stat conditions, and on fluid transport in parallel secretion assays. Acetazolamide abolished forskolin-stimulated HCO_3^- secretion and I_{eq} (Fig. 9A), suggesting a large fraction of the secreted HCO_3^- arises from the intracellular hydration of CO_2 , as suggested previously (Krouse *et al.* 2004).

Formation of the weak acid H_2CO_3 and efflux of HCO_3^- might be expected to stimulate Na^+/H^+ exchangers (NHEs) and other pH_i regulatory mechanisms. However, the NHE inhibitor amiloride (1 mmol l^{-1} ; $\text{IC}_{50} = 24 \mu\text{mol l}^{-1}$) and the NHE1 isoform-specific inhibitor HOE-694 ($20 \mu\text{mol l}^{-1}$; $\text{IC}_{50} = 0.16 \mu\text{mol l}^{-1}$; Counillon *et al.* 1993) did not affect HCO_3^- transport or I_{eq} (Fig. 9B). This suggests pH_i regulation is dependent on the nature of the secretagogue and is mediated by basolateral HCO_3^- influx via NBCe1 and apical H^+ extrusion during forskolin stimulation. Acetazolamide abolished

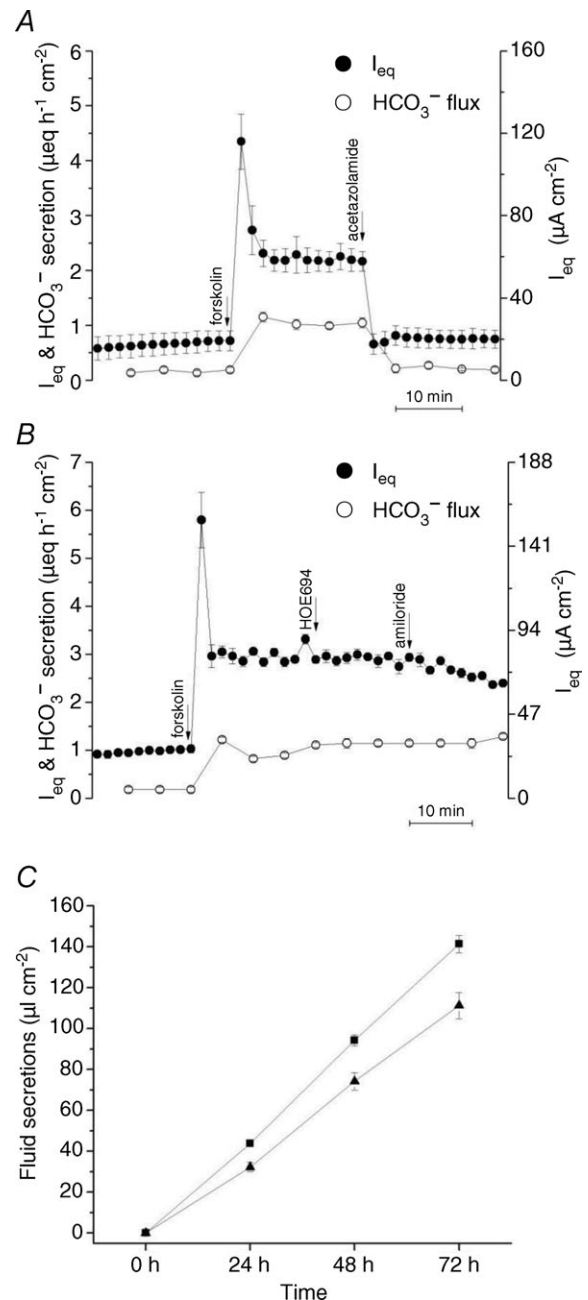


Figure 9. Effect of acetazolamide on anion and fluid secretion by Calu-3 cells

A, the carbonic anhydrase inhibitor acetazolamide ($100 \mu\text{mol l}^{-1}$) abolished forskolin-stimulated secretion ($n = 6$). B, sequential addition of the NHE inhibitors HOE694 ($10 \mu\text{mol l}^{-1}$) and amiloride (1 mmol l^{-1}) to the basolateral side had no effect on I_{eq} or HCO_3^- secretion ($n = 3$). C, acetazolamide caused a small reduction in forskolin-stimulated fluid secretion by Calu-3 cells. \blacksquare , without acetazolamide; \blacktriangle , with acetazolamide ($n = 6$). Means \pm SEM.

forskolin-stimulated I_{eq} (Fig. 9A) but only inhibited fluid secretion by 27% (Fig. 9C).

Origin of the basal I_{eq} and HCO_3^- secretion

Calu-3 monolayers have basal currents of $0.5\text{--}1.0 \mu\text{eq cm}^{-2} \text{h}^{-1}$; however, the nature of this constitutive transport remains uncertain. Since Calu-3 cells express purinergic (Communi *et al.* 1999) and adenosine receptors (Cobb *et al.* 2002) and respond to prostaglandins (Palmer *et al.* 2006b), we examined whether these autocrine signals might be responsible for the basal current. I_{eq} and HCO_3^- transport were unaffected by adding apyrase (10 units ml^{-1}) to metabolize ATP released from the cells, 8-SPT (100 $\mu\text{mol l}^{-1}$) to prevent activation of A2B adenosine receptors, or indomethacin (100 $\mu\text{mol l}^{-1}$) to inhibit prostaglandin synthesis (Fig. 10A–C).

We then examined the role of CFTR and whether there is tonic adenylyl cyclase activity. GlyH-101 (100 $\mu\text{mol l}^{-1}$), which blocks the CFTR channel with an $\text{IC}_{50} \approx 5 \mu\text{mol l}^{-1}$ at -60 mV (Muanprasat *et al.* 2004), strongly inhibited both basal I_{eq} and HCO_3^- transport (Fig. 11).

These results suggest CFTR mediates basal secretion. As a further test for the involvement of CFTR, the dependence of basal current on PKA was investigated. Adding 100 $\mu\text{mol l}^{-1}$ Rp-cAMPS (Rp-adenosine-3',5'-cyclic mono-phosphorothioate triethylamine salt; IC_{50} for inhibition of PKA = 4.9 $\mu\text{mol l}^{-1}$), a membrane-permeant competitive inhibitor of PKA, reduced basal I_{eq} and HCO_3^- secretion by 63% and 88%, respectively (Fig. 11B), evidence that much of the basal secretion is mediated by PKA in resting cells and can be rapidly down-regulated by a phosphatase when PKA is inhibited.

The sensitivity of basal current to PKA inhibitors implies constitutive elevation of cAMP, which may be localized near the apical membrane. There are nine conventional membrane-bound adenylyl cyclases, and one soluble isoform is stimulated by HCO_3^- and proposed to function as a HCO_3^- sensor in various cells (Chen *et al.* 2000), including Calu-3 (Wang *et al.* 2005). Inhibitors were used to examine the role of these adenylyl cyclases. An antagonist of conventional membrane-bound adenylyl cyclases, MDL-12330A (*cis-N*-(2-phenylcyclopentyl) azacyclotridec-1-en-2-amine; Guellaen *et al.* 1977), reduced I_{eq} and HCO_3^- secretion by 68% and 100%, respectively (200 $\mu\text{mol l}^{-1}$; $\text{IC}_{50} < 10 \mu\text{mol l}^{-1}$; Fig. 11C). Since Ca^{2+} -activated adenylyl cyclase might stimulate CFTR, 2-APB (100 $\mu\text{mol l}^{-1}$), a non-specific inhibitor of store-operated Ca^{2+} entry, was also tested (Fig. 11D). Remarkably, 2-APB was a potent inhibitor of basal anion secretion, reducing I_{eq} and HCO_3^- secretion 65–90%. This suggests the membrane-bound adenylyl cyclase is

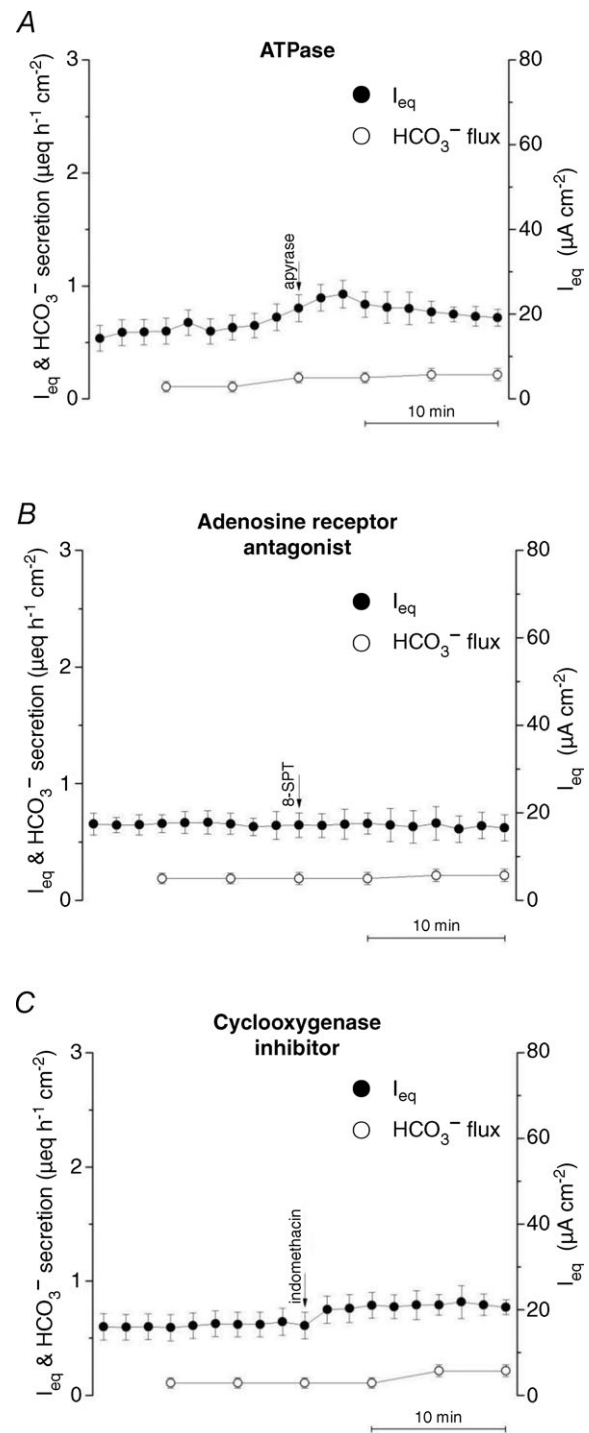


Figure 10. Effects of autocrine signalling inhibitors on I_{eq} and HCO_3^- secretion

Adding A, the ATPase apyrase (10 units ml^{-1}) ($n = 3$) or B, the adenosine receptor antagonist 8-SPT (100 $\mu\text{mol l}^{-1}$) ($n = 3$) apically to block purinergic signalling had no effect on basal I_{eq} or HCO_3^- secretion. C, the cyclo-oxygenase inhibitor indomethacin (100 $\mu\text{mol l}^{-1}$) did not inhibit I_{eq} or HCO_3^- secretion when added bilaterally ($n = 3$). ●, I_{eq} ; ○, HCO_3^- secretion ($n = 3$ for each condition; means \pm SEM).

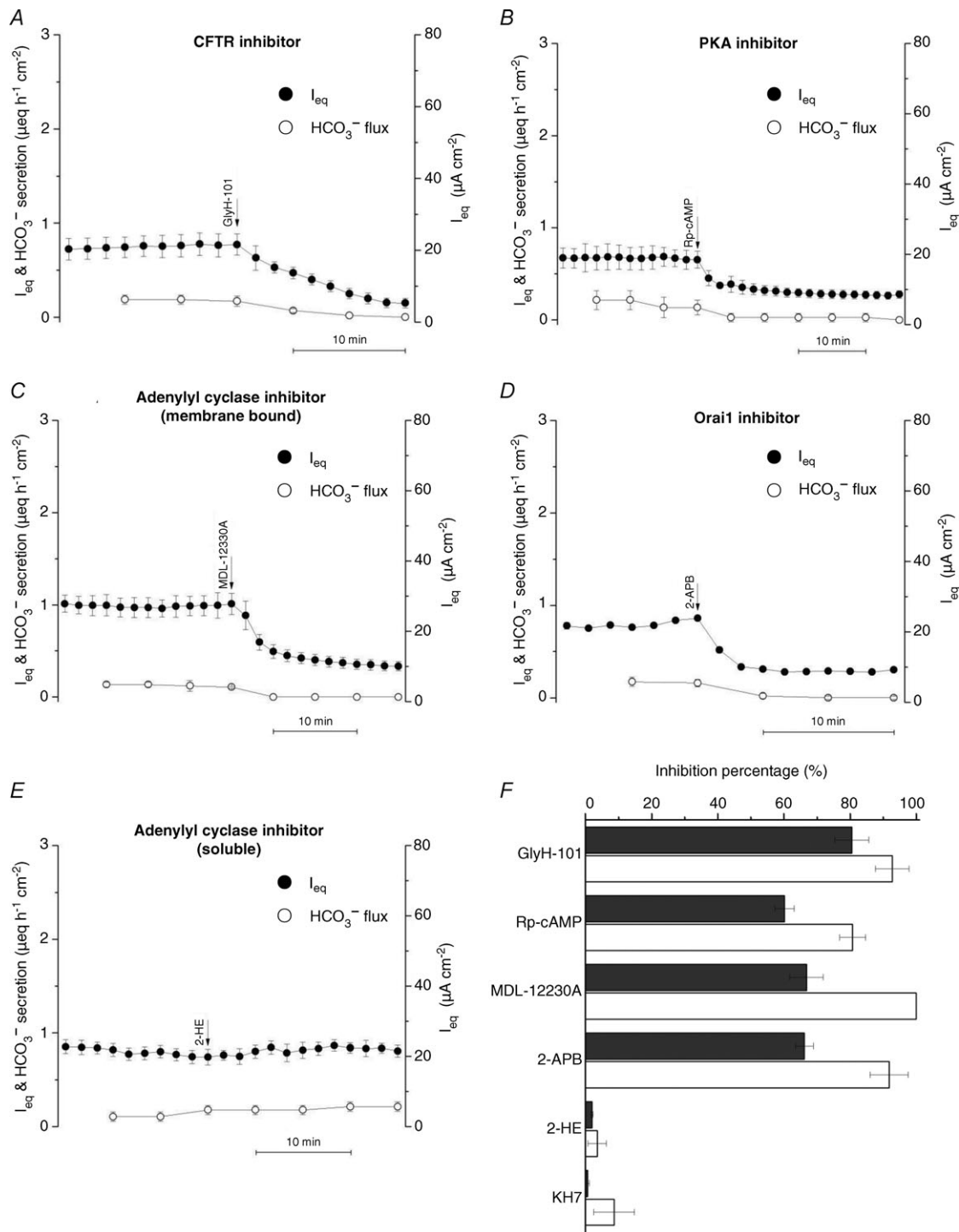


Figure 11. Inhibitor effects suggest basal I_{eq} and HCO_3^- secretion depend on CFTR and on Ca^{2+} -dependent, membrane-bound adenylyl cyclase activity, but not on HCO_3^- -stimulated soluble adenylyl cyclase

A, basal I_{eq} was abolished by apical addition of the CFTR open channel blocker GlyH-101 ($100 \mu\text{mol l}^{-1}$, $n = 4$). B, basal I_{eq} and net HCO_3^- secretion were inhibited by bilateral addition of $200 \mu\text{mol l}^{-1}$ Rp-cAMPS, a competitive inhibitor of cAMP-dependent PKA ($n = 4$). C, basal I_{eq} and HCO_3^- secretion were reduced by basolateral MDL-12230A ($200 \mu\text{mol l}^{-1}$), an inhibitor of membrane-bound adenylyl cyclase ($n = 4$). D, inhibition of basal I_{eq} and HCO_3^- secretion by apical 2-APB ($100 \mu\text{mol l}^{-1}$), an inhibitor of store-operated Ca^{2+} channels ($n = 3$). E, an inhibitor of HCO_3^- -stimulated soluble isoform of adenylyl cyclase, 2-HE ($20 \mu\text{mol l}^{-1}$), had no effect on I_{eq} or HCO_3^- secretion ($n = 3$ each) when added bilaterally. F, summary of inhibitor effects on basal anion transport. ■, I_{eq} ; □, HCO_3^- secretion.

indeed activated by elevated Ca^{2+} near the membrane. By contrast, bilateral addition of 2-hydroxyestradiol (2-HE; 20–50 $\mu\text{mol l}^{-1}$), an inhibitor of soluble adenylyl cyclase (Fig. 11E), had no effect on basal I_{eq} or HCO_3^- transport. The same negative result was obtained using a chemically unrelated inhibitor KH7 (50 $\mu\text{mol l}^{-1}$, $\text{IC}_{50} = 3\text{--}10 \mu\text{mol l}^{-1}$ *in vivo*; data not shown). The effects of these inhibitors on I_{eq} and HCO_3^- transport are summarized in Fig. 11F. Taken together they suggest the basal current in Calu-3 cells is mediated by CFTR channels which are partially activated by PKA. This tonic activity may be due to local production of cAMP by a membrane-bound adenylyl cyclase in response to store-operated Ca^{2+} entry.

Discussion

Electrogenic HCO_3^- and Cl^- secretion by airway epithelia

Electrogenic HCO_3^- secretion by airway epithelium was initially hypothesized because some of the I_{sc} across dog trachea could not be explained by Cl^- and Na^+ net fluxes measured using radiotracers (Al-Bazzaz & Al-Awqati, 1979). The unidentified component of the I_{sc} was increased by the non-specific phosphodiesterase inhibitor aminophylline and therefore stimulated by cAMP (Al-Bazzaz & Jayaram, 1981). HCO_3^- secretion was later confirmed in human airway cell cultures and shown to be defective in cystic fibrosis (Smith *et al.* 1994). Mechanistic studies of HCO_3^- transport have been complicated by its dependence on other ions, the lack of a useful radiotracer, and the unconserved nature of HCO_3^- itself, which may be synthesized and/or degraded during secretion.

Bumetanide (100 μM) had little effect on fluid secretion by submucosal glands in cat trachea (Corrales *et al.* 1984), which suggests the glands use mechanisms other than NKCC1 unlike airway surface epithelial cells, which are mainly bumetanide-sensitive. Cl^- secretion by freshly isolated equine trachea declined $\sim 70\%$ when CO_2 and HCO_3^- were removed under I_{sc} conditions, suggesting basolateral $\text{HCO}_3^-/\text{Cl}^-$ exchange (Tessier *et al.* 1990). Further evidence for basolateral anion exchange (and apical bicarbonate conductance) was obtained in human nasal primary cells by measuring intracellular pH during extracellular Cl^- replacement (Paradiso *et al.* 2003). In summary, HCO_3^- secretion is stimulated by cAMP and defective in CF airway epithelia, and much of the electrogenic anion secretion is insensitive to bumetanide, although the precise role of HCO_3^- in Cl^- and fluid secretion by airway epithelia is not well understood.

The normal pH of ASL and gland secretions is in the range 6.2–7.2 (Fischer & Widdicombe, 2006). Weakly buffered solutions placed on cultures of surface epithelium

become acidic, and pH falls more rapidly on CF than non-CF monolayers, consistent with a defect in parallel HCO_3^- secretion (Coakley *et al.* 2003). The buffer capacity of gland fluid collected in the presence *vs.* absence of HCO_3^- (14 *vs.* 3.7 mmol l^{-1} at pH 7, respectively) suggests that these secretions normally contain about 10 mmol l^{-1} HCO_3^- (Song *et al.* 2006). Secretions from pig glands are 0.2–0.4 units more acidic when secreted in the presence of CFTR inhibitors, mimicking the low pH seen with CF glands (Song *et al.* 2006). A reduction in the HCO_3^- concentration and pH of ASL in CF may inhibit mucociliary clearance by altering the release or micro-rheology of mucus (Quinton, 2010), reducing ciliary beat frequency (Schmid *et al.* 2010) or suppressing innate immunity (Fischer, 2011).

The human airway cell line Calu-3 was used in the present study because it forms polarized monolayers, displays cAMP-stimulated bicarbonate and fluid secretion, expresses the serous cell markers, and responds to gland secretagogues such as vasoactive intestinal peptide and epinephrine (reviewed by Shan *et al.* 2011). The present results confirm that anion and fluid secretion by Calu-3 monolayers are less sensitive to bumetanide than surface epithelial cell primary cultures and resemble cat tracheal glands in this regard (Corrales *et al.* 1984). Although a systematic comparison of the secretion by Calu-3 and human submucosal gland cells remains to be carried out, this result implies that Calu-3 is a useful model for cAMP-stimulated secretion by submucosal gland serous cells although it lacks apical Ca^{2+} -activated Cl^- conductance (Moon *et al.* 1997).

Results consistent with previous studies

Some results in this study can be explained by the current model for Calu-3 cells, which is based on tracer flux and inhibitor studies under I_{sc} conditions (Devor *et al.* 1999), pH-stat experiments (Krouse *et al.* 2004) and fluid secretion measured using a virtual gland technique (Irokawa *et al.* 2004). According to that scheme, I_{sc} is mediated by electrogenic HCO_3^- transport and results from Na^+ -coupled HCO_3^- basolateral entry and apical exit through CFTR channels (Kreindler *et al.* 2006). This section relates the present results obtained under mostly open-circuit, pH-stat conditions with those earlier studies of I_{sc} .

I_{sc} is mediated by electrogenic HCO_3^- transport. The rate of HCO_3^- secretion measured in the present study by automated pH-stat was equal to the simultaneously measured I_{sc} , and both were stimulated by forskolin and abolished by the CFTR inhibitor Inh-172. Close agreement between I_{sc} and HCO_3^- flux is consistent with previous studies of unstimulated (Lee *et al.* 1998) and forskolin-stimulated

Calu-3 monolayers (Devor *et al.* 1999). The $^{36}\text{Cl}^-$ net fluxes measured under open-circuit conditions in Table 1 suggest that membrane hyperpolarization leads to a discrepancy between I_{sc} and HCO_3^- net flux, as suggested previously during stimulation with 1-EBIO (Devor *et al.* 1999). Although forskolin also induced some Cl^- secretion in the present study, this is expected since current flowing through shunt pathways would hyperpolarize the basolateral membrane under open-circuit conditions in concert with apical depolarization (Tamada *et al.* 2001). Thus, the present results extend earlier findings to open-circuit conditions that would exist during fluid transport.

The present results with H^+ transport inhibitors suggest HCO_3^- secretion is actually $\sim 30\%$ higher than the net flux measured by pH-stat. Proton secretion by H^+/K^+ -ATPase has been demonstrated previously during 1-EBIO stimulation (Krouse *et al.* 2004) but was not observed in the present work. The different results obtained using forskolin *vs.* 1-EBIO may be due to their opposite effects on the membrane potential. Forskolin depolarizes the apical membrane (Tamada *et al.* 2001) and should favour electrogenic H^+ efflux pathways whereas 1-EBIO would cause membrane hyperpolarization and favour electroneutral acid secretion. Electrogenic H^+ secretion would be inconspicuous in the present study because it would cause identical reductions in current and HCO_3^- net flux. H^+/K^+ -ATPase activity during 1-EBIO stimulation would consume HCO_3^- without affecting the current and therefore would increase the unidentified component of the I_{sc} , as was demonstrated previously (Krouse *et al.* 2004).

I_{eq} depends on Na^+ and $\text{CO}_2/\text{HCO}_3^-$. Basal and forskolin-stimulated I_{eq} were abolished in Na^+ or HCO_3^- -free solution, consistent with the ionic dependence of I_{sc} reported previously (Devor *et al.* 1999). However, we noticed that $\sim 50\%$ of the HCO_3^- net flux measured under pH-stat conditions persisted despite the nominal absence of Na^+ , suggesting an additional source of HCO_3^- besides NBCe1 (Krouse *et al.* 2004). This flux may reflect carbonic anhydrase-catalysed synthesis and apical efflux since forskolin-stimulated HCO_3^- secretion was abolished by acetazolamide (Fig. 9A), although we cannot exclude basolateral HCO_3^- loading through anion exchangers, which may operate in reversed mode due to the favourable transepithelial HCO_3^- gradient under pH-stat conditions.

Forskolin-stimulated HCO_3^- secretion requires carbonic anhydrase. Acetazolamide abolished forskolin-stimulated I_{sc} and HCO_3^- secretion, as observed previously during stimulation by other secretagogues (Krouse *et al.* 2004). The simplest

explanation for this inhibition is that secreted HCO_3^- must be synthesized in the epithelial cells by carbonic anhydrase to sustain electrogenic secretion, even when NBCe1 is available to mediate basolateral HCO_3^- loading. Acetazolamide inhibition was surprisingly rapid, perhaps because carbonic anhydrase activity and the supply of intracellular bicarbonate are limiting when intracellular pCO_2 and $[\text{HCO}_3^-]$ are low due to $\text{HCO}_3^-/\text{CO}_2$ -free solution on the apical side. It is interesting to consider the role of carbonic anhydrase activity in intracellular pH regulation. Forskolin-stimulated HCO_3^- efflux effectively converts the weak acid H_2CO_3 to a strong acid H^+ , and cells must neutralize this acid load to sustain a high rate of HCO_3^- secretion during steady-state forskolin stimulation. Basolateral HCO_3^- entry via NBCe1 probably mediates most of this pH_i regulation, as occurs during recovery from ammonium-induced acid loads (Inglis *et al.* 2002). The use of basolateral HCO_3^- entry to neutralize intracellular H^+ may generate CO_2 that can be reused for carbonic anhydrase-catalysed HCO_3^- synthesis, and this may be important when intracellular CO_2 and HCO_3^- are low and rate limiting. Future studies should examine whether the sensitivity to acetazolamide is a universal feature of HCO_3^- secretion or a consequence of using pH-stat conditions.

Further evidence that CFTR mediates apical membrane HCO_3^- and Cl^- conductance. When the basolateral membrane was permeabilized using nystatin and an apical-to-basolateral HCO_3^- gradient was imposed, subsequent addition of forskolin produced a (reversed) I_{sc} across control monolayers that was sensitive to the inhibitor CFTR_{inh}-172. Although GlyH-101 has also been shown to inhibit the Cl^- channel/exchanger Slc26a9 (Bertrand *et al.* 2009), the anion exchangers Slc26a3, -a6 and -a11 (Stewart *et al.* 2011), and mitochondrial function (Kelly *et al.* 2010), similar results were obtained using CFTR knock-down cells. Together these results demonstrate the HCO_3^- conductance of CFTR under these conditions, consistent with previous studies of Calu-3 monolayers (Illek *et al.* 1997; Tamada *et al.* 2001; Krouse *et al.* 2004) and with the single channel $P_{\text{HCO}_3^-}/P_{\text{Cl}^-}$ permeability ratio, which ranges between 0.13 and 0.26 (e.g. 0.13, Gray *et al.* 1990; 0.26, Poulsen *et al.* 1994; 0.16, Hanrahan *et al.* 1994; and 0.25, Linsdell *et al.* 1997). Various factors could influence permeability of the CFTR pore to Cl^- and HCO_3^- . The pore is partially blocked by intracellular anions and permeability is enhanced when extracellular Cl^- is replaced with $[\text{HCO}_3^-]$ (Li *et al.* 2011). $P_{\text{HCO}_3^-}/P_{\text{Cl}^-}$ may also be modulated through the WNK1-OSR1/SPAK kinase pathway during stimulated secretion (Park *et al.* 2010).

Forskolin-stimulated I_{sc} was less affected by shRNA than CFTR protein expression, consistent with studies

using a different CFTR-deficient Calu-3 cell line (MacVinish *et al.* 2007). Indeed, basal I_{eq} and HCO_3^- flux were similar in control and CFTR-deficient monolayers even though pharmacological studies indicate basal anion secretion is mediated by CFTR. This result would be explained if some of the band C protein that had been knocked down was not on the cell surface, or if the decline in conductance caused by silencing CFTR was partly offset by an increase in driving force.

Modifications to existing models

This section considers how existing models for Calu-3 transport might be revised to accommodate the results from this study, which were obtained under conditions that have not been used previously to study Calu-3 (i.e. open circuit, pH-stat).

1. Fluid and Cl^- secretion are HCO_3^- dependent, but most fluid is driven by the net flux of Cl^- (or NO_3^-). The $[\text{Cl}^-]$ of secretions was $\sim 120 \text{ mmol l}^{-1}$, or about 4-fold higher than the $[\text{HCO}_3^-]$. This implies that most fluid secretion is driven by transepithelial Cl^- transport rather than HCO_3^- flux during forskolin stimulation despite the fact that active Cl^- transport is not detected (Devor *et al.* 1999), and the I_{sc} can be fully explained by net HCO_3^- flux (Fig. 1). We note, however, that a very low rate of Cl^- transport would be sufficient to sustain fluid secretion at the observed rate and it is difficult to detect a small net flux when it is the difference between two large unidirectional fluxes measured across different monolayers (see section 3 below).

A related finding was that much of the Cl^- transport that drives fluid secretion is independent of NKCC1. This conclusion was based on anion selectivity and pharmacological data. Robust fluid secretion was observed for 24 h when the basolateral side was bathed with nominally Cl^- -free solution containing NO_3^- , which does not bind to the highly selective anion site on NKCC transporters and therefore is not transported (Kinne *et al.* 1986). Further evidence for NKCC1-independent Cl^- entry is the relative insensitivity of fluid secretion to bumetanide. These results suggest other basolateral Cl^- entry pathways such as anion exchangers are important for fluid secretion. NO_3^- is carried by many anion exchangers including AE2 (Humphreys *et al.* 1994).

Although HCO_3^- is secreted by Calu-3 cells under open-circuit conditions, its concentration in the secreted fluid is low compared with Cl^- . If anion secretion drives fluid transport, the higher concentration of Cl^- suggests that it provides more of the osmotic driving force for fluid secretion. Some of the HCO_3^- entering via NBCe1 returns to the basolateral side, apparently by exchanging for Cl^- (or NO_3^-). The anion exchangers that mediate this baso-

lateral Cl^- loading were not identified at the molecular level in the present study; however, AE2 is the most likely candidate since it is expressed at the basolateral membrane of Calu-3 cells (Loffing *et al.* 2000). Recent studies of an AE2-deficient Calu-3 cell line indicate that AE2 mediates essentially all $\text{Cl}^-/\text{HCO}_3^-$ exchange at the basolateral membrane and plays an important role in fluid secretion; nevertheless, there is another bumetanide-insensitive mechanism for Cl^- loading at the basolateral membrane in AE2 cells that remains to be identified (Huang *et al.* submitted).

Basolateral anion exchange was demonstrated in the present study by permeabilizing the apical membrane, imposing an apical-to-basolateral HCO_3^- gradient, and examining the effect of anions in the basolateral solution on the HCO_3^- flux. Nystatin is Na^+ permeable, thus apical nystatin permitted apical Na^+ entry and produced a large transepithelial current, which was mediated by the basolateral sodium pump since it was ouabain sensitive. This response had variable kinetics due to the use of different batches of nystatin (compare Fig. 8A and B with Fig. 8C). We speculate that this results from variations in the aggregation state of nystatin and rate of incorporation into the apical membrane. The time course of permeabilization did not affect our conclusions regarding anions on the 'trans' side, however, because Na^+ currents were allowed to stabilize before studying the effects of basolateral (trans) anions on HCO_3^- flux.

2. Calu-3 secretions are only weakly alkaline. HCO_3^- -driven fluid transport was expected to generate strongly alkaline secretions having $\text{pH} > 8$; however, the maximal pH achieved during forskolin stimulation in the present experiments was ~ 7.6 . The calculated $[\text{HCO}_3^-]$ in secretions was slightly higher than in the basolateral medium (33 vs. 25 mmol l^{-1}), and higher apical $[\text{HCO}_3^-]$ was achieved by parental Calu-3 monolayers, which have higher CFTR expression ($\sim 50 \text{ mM } [\text{HCO}_3^-]$; D. Kim, unpublished observations, Fig. 2A); nevertheless, secretions were always less alkaline than expected for fluid driven by HCO_3^- transport. The values obtained with parental cells were generally consistent with previous studies in a virtual gland preparation (74 $\text{mM } \text{HCO}_3^-$ (Irokawa *et al.* 2004), and cyclophilin B shRNA control Calu-3 cells cultured on transwells (60 mM ; Garnett *et al.* 2011). Silencing CFTR reduced the $[\text{HCO}_3^-]$ of secretions by $\sim 50\%$ in the present study, whereas CFTR knock-down had no effect on the pH and HCO_3^- concentration in previous studies (Garnett *et al.* 2011), perhaps because those knock-down cells had higher residual CFTR expression (28% vs. $< 5\%$). The $[\text{HCO}_3^-]$ is reduced in CF gland secretions (Song *et al.* 2006), albeit from a lower starting value (i.e. 13.8 mmol l^{-1} vs. 3.5 mmol l^{-1} $[\text{HCO}_3^-]$ in non-CF vs. CF glands, respectively).

In the present study, silencing CFTR expression caused reductions in the volume and total Cl^- content by 10-fold and also caused a 2-fold decrease in the $[\text{HCO}_3^-]$ of the secretions. Similar changes in CF airways may contribute to disease symptoms by altering mucus release or rheology, innate immunity or ciliary beating (Shan *et al.* 2011).

3. A low rate of net Cl^- secretion is sufficient to drive fluid secretion. HCO_3^- secretion accounted for $\sim 40\%$ of the I_{eq} under pH-stat conditions. The remainder ($1.5 \mu\text{eq cm}^{-2} \text{h}^{-1}$) was carried by Cl^- , as revealed by measuring $^{36}\text{Cl}^-$ fluxes under the same conditions. Nevertheless, Cl^- net flux was negligible during previous short-circuit current experiments (Devor *et al.* 1999) and under open-circuit conditions in the present study (Table 1), making it difficult to understand how Calu-3 monolayers could produce Cl^- -rich fluid. However, a net Cl^- flux of $0.21 \mu\text{eq cm}^{-2} \text{h}^{-1}$ would be sufficient to account for the Cl^- content of secretions, and such low rates could not be determined reliably in Ussing chambers. In preliminary tracer experiments performed in Transwells over 24 h, a net Cl^- flux of $0.23 \mu\text{eq cm}^{-2} \text{h}^{-1}$ was observed; therefore this low rate of Cl^- transport could drive fluid secretion (J. Shan, personal observation).

Elevating mucosal HCO_3^- to 50 mmol l^{-1} with 25 mmol l^{-1} $[\text{HCO}_3^-]$ on the serosal side increased the forward and back fluxes of $^{36}\text{Cl}^-$ (Table 4). Although the mechanism of this increase was not studied in detail, it may be secondary to an increase in intracellular pH. The basolateral anion exchanger AE2 is stimulated 5- to 10-fold by raising pH_i from 6.8 to 7.3 (Alper, 2009). Increasing its turnover by raising pH_i should increase $^{36}\text{Cl}^-$ flux in both directions if the basolateral anion exchange is rate limiting.

Cl^- , HCO_3^- and fluid secretion by Calu-3

The present results suggest a revised model of fluid and electrolyte secretion by Calu-3 cells (Fig. 12). Most fluid secretion is driven by Cl^- secretion and 50–70% of the basolateral Cl^- loading occurs by anion exchange, which is increased during forskolin-stimulated secretion. This scheme differs from a model in which NKCC mediates basolateral Cl^- entry (Devor *et al.* 1999). We hypothesize that basolateral Cl^- loading via basolateral anion exchange increases during forskolin stimulation, in contrast to another recent model for Calu-3 in which forskolin stimulation was proposed to inhibit basolateral anion exchange (Garnett *et al.* 2011).

Forskolin stimulates a large transient current which is abolished in Cl^- -free solution and therefore probably mediated by apical Cl^- and basolateral K^+ efflux. While the decline in intracellular Cl^- activity would favour basolateral anion exchange, cell shrinkage produced by the

loss of these solutes may trigger a volume regulatory increase and stimulation of Cl^- entry through NKCC1 (Jiang *et al.* 1997). In this scheme for Calu-3 cells, most apical HCO_3^- efflux is sustained by intracellular HCO_3^- synthesis, which is catalysed by carbonic anhydrase. The acid load produced by forskolin-stimulated HCO_3^- efflux may be neutralized by HCO_3^- entry through NBCe1, whereas H^+ extrusion via electroneutral NHE1 (Cuthbert *et al.* 2003) and H^+/K^+ -ATPase (Krouse *et al.* 2004) mediate pH_i regulation during the response to hyperpolarizing secretagogues.

Calu-3 monolayers had significant basal I_{eq} and HCO_3^- secretion. Basal activity was sensitive to inhibitors of CFTR (GlyH-101), PKA catalytic subunit (Rp-cAMPS) and membrane-bound adenylyl cyclase (MDL-12330A). Adenylyl cyclase may be constitutively activated by Ca^{2+} entry through the store-operated Ca^{2+} entry channel Orai1. A similar mechanism would explain the high basal activity of CFTR in other tissues such as the sweat duct (Quinton, 1983) and small airways (Wang *et al.* 2006). The present results do not allow discrimination of

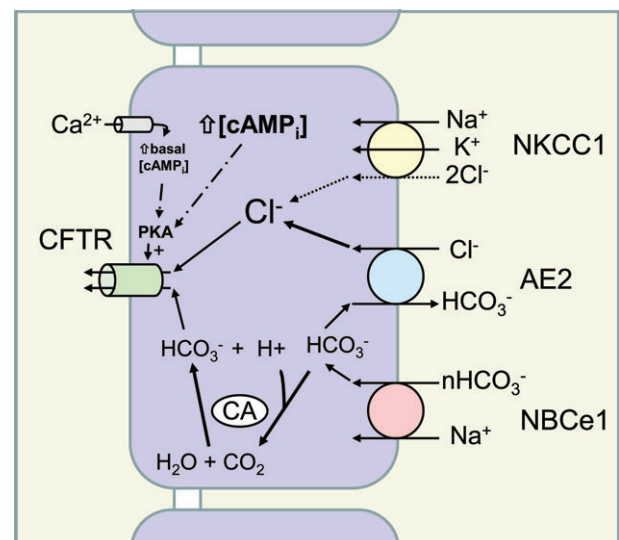


Figure 12. Scheme for anion transport by Calu-3 cells under the conditions used in this study

In resting cells, an apical Ca^{2+} microdomain produced by store-operated Ca^{2+} entry causes partial activation of CFTR through stimulation of membrane-bound adenylyl cyclase and local elevation of $[\text{cAMP}]$. Secretagogues that further elevate $[\text{cAMP}]$ stimulate apical Cl^- and HCO_3^- efflux, creating an acid load that may further increase CFTR open probability (Chen *et al.* 2009). Regulation of pH_i by HCO_3^- that enters via NBCe1 provides CO_2 for bicarbonate synthesis by carbonic anhydrase, which sustains HCO_3^- secretion. Most bicarbonate entering via NBCe1 is recycled basolaterally by anion exchange during Cl^- loading. Not shown in this scheme are other anion exchangers and Na^+/H^+ exchangers that are active under other conditions; i.e. Na^+/H^+ exchange is likely to mediate pH_i regulation during stimulation by secretagogues that hyperpolarize the basolateral membrane.

conductances that are strictly dependent on CFTR activity (Bertrand *et al.* 2009).

Relevance to other epithelia

Early work identified cAMP-stimulated anion conductance (Klyce & Wong, 1977; Shorofsky *et al.* 1983; Welsh *et al.* 1983) and demonstrated basolateral Cl^- loading by furosemide- and bumetanide-sensitive cotransporters in native tissues (Frizzell *et al.* 1979) and cell lines (Dharmasathaphorn *et al.* 1985), including airway epithelial cell cultures (Widdicombe *et al.* 1985). Calu-3 is used as a model for submucosal gland serous cells, whereas only surface epithelial cells have been studied extensively in primary culture. Perhaps the best evidence that the Calu-3 model shown in Fig. 12 may apply to glands in native tissue comes from early studies of cat trachea, where bumetanide (100 μM) caused negligible inhibition of gland secretion (see Fig. 7 in Corrales *et al.* 1984). More recent studies of droplets secreted under oil also indicate a substantial bumetanide-insensitive component in gland fluid secretion (Joo *et al.* 2002). Approximately half of the vasoactive intestinal peptide (VIP)-stimulated fluid secretion by pig and human glands was insensitive to bumetanide, and replacing CO_2 /bicarbonate with Hepes (which should inhibit basolateral Cl^- loading by anion exchangers) reduced secretion rate by 67%; thus, HCO_3^- removal caused greater inhibition than bumetanide addition. In summary, the present Calu-3 results are consistent with some previous studies and suggest fluid secretion by glands is less dependent on NKCC compared with other epithelia such as airway surface cells.

Acetazolamide abolished forskolin-stimulated HCO_3^- secretion and strongly inhibited I_{eq} in the present study, evidence for the involvement of carbonic anhydrase during HCO_3^- secretion (Cuthbert *et al.* 2003; Krouse *et al.* 2004; Smith & Welsh, 1992). Catalysing HCO_3^- synthesis may supply HCO_3^- for secretion while HCO_3^- entry via NBCe1 maintains pH_i while promoting basolateral HCO_3^- recycling and Cl^- entry by exchangers.

This paper presents a model for secretion by Calu-3 cells in which basolateral anion exchange mediates a major portion of Cl^- loading during secretion. A similar mechanism may explain the surprisingly weak sensitivity of gland secretion to bumetanide that has been reported in native airway tissues (e.g. Corrales *et al.* 1984). Basolateral anion exchangers such as AE2 are expressed in Calu-3 (Loffing *et al.* 2000) and intestinal epithelia (Alper, 2009), and intestinal fluid secretion is defective in $\text{Ae}2^{-/-}$ knock-out mice (Gawenis *et al.* 2010). Studies of an AE2 knock-down cell line in the following companion paper provide direct evidence for the role of this anion exchanger in fluid secretion by Calu-3 cells (Huang *et al.* 2012).

References

- Acevedo M & Steele LW (1993). Na^+/H^+ exchanger in isolated epithelial tracheal cells from sheep. Involvement in tracheal proton secretion. *Exp Physiol* **78**, 383–394.
- Al-Bazzaz F & Jayaram T (1981). Ion transport by canine tracheal mucosa: effect of elevation of cellular calcium. *Exp Lung Res* **2**, 121–130.
- Al-Bazzaz FJ & Al-Awqati Q (1979). Interaction between sodium and chloride transport in canine tracheal mucosa. *J Appl Physiol* **46**, 111–119.
- Alper SL (2009). Molecular physiology and genetics of Na^+ -independent SLC4 anion exchangers. *J Exp Biol* **212**, 1672–1683.
- Ballard ST, Trout L, Bebök Z, Sorscher EJ & Crews A (1999). CFTR involvement in chloride, bicarbonate, and liquid secretion by airway submucosal glands. *Am J Physiol Lung Cell Mol Physiol* **277**, L694–L699.
- Bertrand CA, Zhang R, Pilewski JM & Frizzell RA (2009). SLC26A9 is a constitutively active, CFTR-regulated anion conductance in human bronchial epithelia. *J Gen Physiol* **133**, 421–438.
- Boucher RC (2003). Regulation of airway surface liquid volume by human airway epithelia. *Pflügers Arch* **445**, 495–498.
- Chen J-H, Cai Z & Sheppard DN (2009). Direct sensing of intracellular pH by the cystic fibrosis transmembrane conductance regulator (CFTR) Cl^- channel. *J Biol Chem* **284**, 35495–35506.
- Chen Y, Cann MJ, Litvin TN, Iourgenko V, Sinclair ML, Levin LR & Buck J (2000). Soluble adenylyl cyclase as an evolutionarily conserved bicarbonate sensor. *Science* **289**, 625–628.
- Coakley RD, Grubb BR, Paradiso AM, Gatzky JT, Johnson LG, Kreda SM, O'Neal WK & Boucher RC (2003). Abnormal surface liquid pH regulation by cultured cystic fibrosis bronchial epithelium. *Proc Natl Acad Sci U S A* **100**, 16083–16088.
- Cobb BR, Ruiz F, King CM, Fortenberry J, Greer H, Kavacs T, Sorscher EJ & Clancy JP (2002). A_2 adenosine receptors regulate CFTR through PKA and PLA_2 . *Am J Physiol Lung Cell Mol Physiol* **282**, L12–L25.
- Communi D, Paindavoine P, Place GA, Parmentier M & Boeynaems J-M (1999). Expression of P2Y receptors in cell lines derived from the human lung. *Br J Pharmacol* **127**, 562–568.
- Corrales RJ, Nadel JA & Widdicombe JH (1984). Source of the fluid component of secretions from tracheal submucosal glands in cats. *J Appl Physiol* **56**, 1076–1082.
- Counillon L, Scholz W, Lang HJ & Pouyssegur J (1993). Pharmacological characterization of stably transfected Na^+/H^+ antiporter isoforms using amiloride analogs and a new inhibitor exhibiting anti-ischemic properties. *Mol Pharmacol* **44**, 1041–1045.
- Cuthbert AW, Supuran CT & MacVinish LJ (2003). Bicarbonate-dependent chloride secretion in Calu-3 epithelia in response to 7,8-benzoquinoline. *J Physiol* **551**, 79–92.
- Devor DC, Singh AK, Lambert LC, DeLuca A, Frizzell RA & Bridges RJ (1999). Bicarbonate and chloride secretion in Calu-3 human airway epithelial cells. *J Gen Physiol* **113**, 743–760.

- Dharmasathaphorn K, Mandel KG, Masui H & McRoberts JA (1985). Vasoactive intestinal polypeptide-induced chloride secretion by a colonic epithelial cell line. *J Clin Invest* **75**, 462–471.
- Fischer H (2011). Function of proton channels in lung epithelia. *Wiley Interdiscip Rev Membr Transp Signal* **1**, 247–258.
- Fischer H & Widdicombe JH (2006). Mechanisms of acid and base secretion by the airway epithelium. *J Membr Biol* **211**, 139–150.
- Fischer H, Widdicombe JH & Illek B (2002). Acid secretion and proton conductance in human airway epithelium. *Am J Physiol Cell Physiol* **282**, C736–C743.
- Frizzell RA, Field M & Schultz SG (1979). Sodium-coupled chloride transport by epithelial tissues. *Am J Physiol Renal Fluid Electrol Physiol* **236**, F1–F8.
- Frizzell RA & Hanrahan JW (2011). Physiology of chloride and fluid secretion. In *Cystic Fibrosis: Molecular Basis, Physiological Changes, and Therapeutic Strategies*, eds. Riordan JR, Boucher RC & Quinton PM. Cold Spring Harbor Press, Cold Spring.
- Garnett JP, Hickman E, Burrows R, Hegyi P, Tiszlavicz L, Cuthbert AW, Fong P & Gray MA (2011). Novel role for pendrin in orchestrating bicarbonate secretion in cystic fibrosis transmembrane conductance regulator (CFTR)-expressing airway serous cells. *J Biol Chem* **286**, 41069–41082.
- Gawenis LR, Bradford EM, Alper SL, Prasad V & Schull GE (2010). AE2 Cl⁻/HCO₃⁻ exchanger is required for normal cAMP-stimulated anion secretion in murine proximal colon. *Am J Physiol Gastrointest Liver Physiol* **298**, G493–G503.
- Gray MA, Pollard CE, Harris A, Coleman L, Greenwell JR & Argent BE (1990). Anion selectivity and block of the small conductance chloride channel on pancreatic duct cells. *Am J Physiol Cell Physiol* **259**, C752–C761.
- Guellaen G, Mahu JL, Mavier P, Berthelot P & Hanoune J (1977). RMI 12330 A, an inhibitor of adenylate cyclase in rat liver. *Biochim Biophys Acta* **484**, 465–475.
- Hanrahan JW, Tabcharani JA, Chang X-B & Riordan JR (1994). A secretory Cl channel from epithelial cells studied in heterologous expression systems. In *Electrogenic Cl⁻ Transporters in Biological Membranes*, ed. Gersenker G, pp. 193–220. Springer Verlag, Berlin.
- Haws C, Finkbeiner WE, Widdicombe JH & Wine JJ (1994). CFTR in Calu-3 human airway cells: channel properties and role in cAMP-activated Cl⁻ conductance. *Am J Physiol Lung Cell Mol Physiol* **266**, L502–L512.
- Huang J, Shan J, Alper SL & Hanrahan JW (2011). Secretion by the human airway epithelial cell line Calu-3 depends on basolateral chloride loading by AE2. *Proc Physiol Soc* **23**, 160.
- Huang J, Shan J, Kim D, Liao J, Evagelidis A, Alper SL & Hanrahan JW (2012). Basolateral chloride loading by AE2: role in fluid secretion by the human airway epithelial cell line Calu-3. *J Physiol* **590**, 5299–5316.
- Humphreys BD, Jiang L, Chernova MN & Alper SL (1994). Functional characterization and regulation by pH of murine AE2 anion exchanger expressed in *Xenopus* oocytes. *Am J Physiol Cell Physiol* **267**, C1295–C1307.
- Illek B, Yankaskas JR & Machen TE (1997). cAMP and genistein stimulate HCO₃⁻ conductance through CFTR in human airway epithelia. *Am J Physiol Lung Cell Mol Physiol* **272**, L752–L761.
- Inglis SK, Finlay L, Ramminger SJ, Richard K, Ward MR, Wilson SM & Olver RE (2002). Regulation of intracellular pH in Calu-3 human airway cells. *J Physiol* **538**, 527–539.
- Inglis SK, Wilson SM & Olver RE (2003). Secretion of acid and base equivalents by intact distal airways. *Am J Physiol Lung Cell Mol Physiol* **284**, L855–L862.
- Iovannisci D, Illek B & Fischer H (2010). Function of the HVCN1 proton channel in airway epithelia and a naturally occurring mutation, M91T. *J Gen Physiol* **136**, 35–46.
- Irokawa T, Krouse ME, Joo NS, Wu JV & Wine JJ (2004). A 'virtual gland' method for quantifying epithelial fluid secretion. *Am J Physiol Lung Cell Mol Physiol* **287**, L784–L793.
- Ishiguro H, Steward MC, Naruse S, Ko SB, Goto H, Case RM, Kondo T & Yamamoto A (2009). CFTR functions as a bicarbonate channel in pancreatic duct cells. *J Gen Physiol* **133**, 315–326.
- Jiang L, Chernova MN & Alper SL (1997). Secondary regulatory volume increase conferred on *Xenopus* oocytes by expression of AE2 anion exchanger. *Am J Physiol Cell Physiol* **272**, C191–C202.
- Joo NS, Saenz Y, Krouse ME & Wine JJ (2002). Mucus secretion from single submucosal glands of pig. Stimulation by carbachol and vasoactive intestinal peptide. *J Biol Chem* **277**, 28167–28175.
- Kartner N & Riordan JR (1998). Characterization of polyclonal and monoclonal antibodies to cystic fibrosis transmembrane conductance regulator. *Methods Enzymol* **292**, 629–652.
- Kelly M, Trudel S, Brouillard F, Bouillaud F, Colas J, Nguyen-Khoa T, Ollero M, Edelman A & Fritsch J (2010). Cystic fibrosis transmembrane regulator inhibitors CFTR(inh)-172 and GlyH-101 target mitochondrial functions, independently of chloride channel inhibition. *J Pharmacol Exp Ther* **333**, 60–69.
- Kim D & Steward MC (2009). The role of CFTR in bicarbonate secretion by pancreatic duct and airway epithelia. *J Med Invest* **56**, 336–342.
- Kinne R, Kinne-Saffran E, Schölermann B & Schütz H (1986). The anion specificity of the sodium-potassium-chloride cotransporter in rabbit kidney outer medulla: studies on medullary plasma membranes. *Pflügers Arch* **407**, S168–S173.
- Klyce SD & Wong RKS (1977). Site and mode of adrenaline action on chloride transport across the rabbit corneal epithelium. *J Physiol* **266**, 777–799.
- Kreindler JL, Peters KW, Frizzell RA & Bridges RJ (2006). Identification and membrane localization of electrogenic sodium bicarbonate cotransporters in Calu-3 cells. *Biochim Biophys Acta* **1762**, 704–710.
- Krouse ME, Talbott JF, Lee MM, Joo NS & Wine JJ (2004). Acid and base secretion in the Calu-3 model of human serous cells. *Am J Physiol Lung Cell Mol Physiol* **287**, L1274–L1283.
- Kyle H, Ward JPT & Widdicombe JG (1990). Control of pH of airway surface liquid of the ferret trachea *in vitro*. *J Appl Physiol* **68**, 135–140.

- Lee MC, Penland CM, Widdicombe JH & Wine JJ (1998). Evidence that Calu-3 human airway cells secrete bicarbonate. *Am J Physiol Lung Cell Mol Physiol* **274**, L450–L453.
- Lee MG, Choi JY, Luo X, Strickland E, Thomas PJ & Muallem S (1999). Cystic fibrosis transmembrane conductance regulator regulates luminal $\text{Cl}^-/\text{HCO}_3^-$ exchange in mouse submandibular and pancreatic ducts. *J Biol Chem* **274**, 14670–14677.
- Lewis SA, Wills NK & Eaton DC (1978). Basolateral membrane potential of a tight epithelium: ionic diffusion and electrogenic pumps. *J Membr Biol* **41**, 117–148.
- Li MS, Holstead RG, Wang W & Linsdell P (2011). Regulation of CFTR chloride channel macroscopic conductance by extracellular bicarbonate. *Am J Physiol Cell Physiol* **300**, C65–C74.
- Linsdell P, Tabcharani JA, Rommens JM, Hou Y-X, Chang X-B, Tsui L-C, Riordan JR & Hanrahan JW (1997). Permeability of wild-type and mutant cystic fibrosis transmembrane conductance regulator chloride channels to polyatomic anions. *J Gen Physiol* **110**, 355–364.
- Loffing J, Moyer BD, Reynolds D, Shmukler BE, Alper SL & Stanton BA (2000). Functional and molecular characterization of an anion exchanger in airway serous epithelial cells. *Am J Physiol Cell Physiol* **279**, C1016–C1023.
- Luo Y, McDonald K & Hanrahan JW (2009). Trafficking of immature DeltaF508-CFTR to the plasma membrane and its detection by biotinylation. *Biochem J* **419**, 211–219.
- Ma T, Thiagarajah JR, Yang H, Sonawane ND, Folli C, Galiotta LJV & Verkman AS (2002). Thiazolidinone CFTR inhibitor identified by high-throughput screening blocks cholera toxin-induced intestinal fluid secretion. *J Clin Invest* **110**, 1651–1658.
- MacVinish LJ, Cope G, Ropenga A & Cuthbert AW (2007). Chloride transporting capability of Calu-3 epithelia following persistent knockdown of the cystic fibrosis transmembrane conductance regulator, CFTR. *Br J Pharmacol* **150**, 1055–1065.
- Moon S, Singh M, Krouse ME & Wine JJ (1997). Calcium-stimulated Cl^- secretion in Calu-3 human airway cells requires CFTR. *Am J Physiol Lung Cell Mol Physiol* **273**, L1208–L1219.
- Muanprasat C, Sonawane ND, Salinas D, Taddei A, Galiotta LJV & Verkman AS (2004). Discovery of glycine hydrazide pore-occluding CFTR inhibitors: mechanism, structure-activity analysis, and *in vivo* efficacy. *J Gen Physiol* **124**, 125–137.
- Palmer ML, Lee SY, Carlson D, Fahrenkrug S & O'Grady SM (2006). Stable knockdown of CFTR establishes a role for the channel in P2Y receptor-stimulated anion secretion. *J Cell Physiol* **206**, 759–770.
- Paradiso AM, Coakley RD & Boucher RC (2003). Polarized distribution of HCO_3^- transport in human normal and cystic fibrosis nasal epithelia. *J Physiol* **548**, 203–218.
- Park HW, Nam JH, Kim JY, Namkung W, Yoon JS, Lee JS, Kim KS, Venglovecz V, Gray MA, Kim KH & Lee MG (2010). Dynamic regulation of CFTR bicarbonate permeability by $[\text{Cl}^-]_i$ and its role in pancreatic bicarbonate secretion. *Gastroenterology* **139**, 620–631.
- Paunescu TG, Ljubojevic M, Russo LM, Winter C, McLaughlin MM, Wagner CA, Breton S & Brown D (2010). cAMP stimulates apical V-ATPase accumulation, microvillar elongation, and proton extrusion in kidney collecting duct A-intercalated cells. *Am J Physiol Renal Fluid Electrol Physiol* **298**, F643–F654.
- Poulsen JH, Fischer H, Illek B & Machen TE (1994). Bicarbonate conductance and pH regulatory capability of cystic fibrosis transmembrane conductance regulator. *Proc Natl Acad Sci U S A* **91**, 5340–5344.
- Quinton PM (1983). Chloride impermeability in cystic fibrosis. *Nature* **301**, 421–422.
- Quinton PM (2010). Role of epithelial HCO_3^- transport in mucin secretion: lessons from cystic fibrosis. *Am J Physiol Gastrointest Liver Physiol* **299**, C1222–C1233.
- Rasband WS (2011). ImageJ. *National Institutes of Health, Bethesda, Maryland USA* <http://imagej.nih.gov/ij/>, 1997–2011.
- Schmid A, Sutto Z, Schmid N, Novak L, Ivonnet P, Horvath G, Conner G, Fregien N & Salathe M (2010). Decreased soluble adenylyl cyclase activity in cystic fibrosis is related to defective apical bicarbonate exchange and affects ciliary beat frequency regulation. *J Biol Chem* **285**, 29998–30007.
- Shan J, Huang J, Liao J, Robert R & Hanrahan JW (2011). Anion secretion by a model epithelium: More lessons from Calu-3. *Acta Physiol* **202**, 523–531.
- Shen B-Q, Finkbeiner WE, Wine JJ, Mrsny RJ & Widdicombe JH (1994). Calu-3: a human airway epithelial cell line that shows cAMP-dependent Cl^- secretion. *Am J Physiol Lung Cell Mol Physiol* **266**, L493–L501.
- Shorofsky SR, Field M & Fozzard HA (1983). Electrophysiology of Cl^- secretion in canine trachea. *J Membr Biol* **72**, 105–115.
- Smith JJ, Karp PH & Welsh MJ (1994). Defective fluid transport by cystic fibrosis airway epithelia. *J Clin Invest* **93**, 1307–1311.
- Smith JJ & Welsh MJ (1992). cAMP stimulates bicarbonate secretion across normal, but not cystic fibrosis airway epithelia. *J Clin Invest* **89**, 1148–1153.
- Song Y, Salinas D, Nielson DW & Verkman AS (2006). Hyperacidity of secreted fluid from submucosal glands in early cystic fibrosis. *Am J Physiol Cell Physiol* **290**, C741–C749.
- Stewart AK, Shmukler BE, Vandorpe DH, Reimold F, Heneghan JF, Nakakuki M, Akhavein A, Ko S, Ishiguro H & Alper SL (2011). SLC26 anion exchangers of guinea pig pancreatic duct: molecular cloning and functional characterization. *Am J Physiol Cell Physiol* **301**, C289–C303.
- Takeyasu K, Tamkun MM, Renaud KJ & Fambrough DM (1988). Ouabain-sensitive ($\text{Na}^+ + \text{K}^+$)-ATPase activity expressed in mouse L cells by transfection with DNA encoding the α -subunit of an avian sodium pump. *J Biol Chem* **263**, 4347–4354.
- Tamada T, Hug MJ, Frizzell RA & Bridges RJ (2001). Microelectrode and impedance analysis of anion secretion in Calu-3 cells. *JOP* **2**, 219–228.
- Tarran R, Trout L, Donaldson SH & Boucher RC (2006). Soluble mediators, not cilia, determine airway surface liquid volume in normal and cystic fibrosis superficial airway epithelia. *J Gen Physiol* **127**, 591–604.

- Tessier GJ, Traynor TR, Kannan MS & O'Grady SM (1990). Mechanisms of sodium and chloride transport across equine tracheal epithelium. *Am J Physiol Lung Cell Mol Physiol* **259**, L459–L467.
- Wang X, Lytle C & Quinton PM (2006). Predominant constitutive CFTR conductance in small airways. *Resp Res* **6**, 7.
- Wang Y, Lam CS, Wu F, Wang W, Duan Y & Huang P (2005). Regulation of CFTR channels by HCO₃-sensitive soluble adenylyl cyclase in human airway epithelial cells. *Am J Physiol Cell Physiol* **289**, C1145–C1151.
- Welsh MJ, Smith PL & Frizzell RA (1983). Chloride secretion by canine tracheal epithelium: III. Membrane resistances and electromotive forces. *J Membr Biol* **71**, 209–218.
- Widdicombe JH (2002). Regulation of the depth and composition of airway surface liquid. *J Anat* **201**, 313–318.
- Widdicombe JH, Welsh MJ & Finkbeiner WE (1985). Cystic fibrosis decreases the apical membrane chloride permeability of monolayers cultured from cells of tracheal epithelium. *Proc Natl Acad Sci U S A* **82**, 6167–6171.

Author contributions

J.S. and J.W.H.: conception and design of the experiments; J.S., J.L., J.H. and R.R.: collection, analysis and interpretation of data,

M.L.P., S.C.F. and S.M.O.: essential advice and reagents, J.S., S.M.O. and J.W.H.: drafting the article or revising it critically for important intellectual content. The work was conducted in the Cystic Fibrosis Translational Research Centre, Department of Physiology, McGill University. All authors approved the final version for publication.

Acknowledgements

We thank Drs R. Beaulieu (Hôpital Hôtel Dieu) and D. Bowie (McGill University) for access to equipment, J. Riordan (UNC Chapel Hill, NC) and R. Mercer (Washington University, St Louis, MO, USA) for antibodies, W. Marshall (St Francis-Xavier University, Antigonish, NS, Canada) for H³⁶Cl, R. Bridges (Rosalind Franklin University, The Chicago Medical School) and Cystic Fibrosis Foundation Therapeutics Inc. for CFTR inhibitors, and S. Alper (Harvard University) for comments on the manuscript. This study was supported by Cystic Fibrosis Canada, a Seed Grant to J.W.H. from the Canadian Institutes of Health Research program entitled 'Novel Alternatives to Antibiotics', and NIH contract grant AI50494 to S.M.O. J.W.H. is affiliated with the Groupe d'étude des protéines membranaires (GEPROM) and the Groupe de recherche axé sur la structure des protéines (GRASP).